# NATIONAL ADVISORY COMMITTEE FOR AERONAUTICS

TECHNICAL NOTE

No. 1050

## WIND-TUNNEL INVESTIGATION OF END-PLATE EFFECTS OF HORIZONTAL TAILS ON A VERTICAL TAIL COMPARED WITH AVAILABLE THEORY

By Harry E. Murray

Langley Memorial Aeronautical Laboratory
Langley Field, Va.

FOR REFERENCE




Washington
April 1946

NATIONAL ADVISORY COMMITTEE FOR AERONAUTICS

TECHNICAL NOTE NO. 1050

# WIND-TUNNEL INVESTIGATION OF END-PLATE EFFECTS OF HORIZONTAL TAILS ON A VERTICAL TAIL COMPARED WITH AVAILABLE THEORY

By Harry E. Murray

## SUMMARY

A vertical-tail model with stub fuselage was tested in combination with various simulated horizontal tails to determine the effect of horizontal-tail span and location on the aerodynamic characteristics of the vertical tail. Available theoretical data on end-plate effects were collected and presented in the form most suitable for design purposes.

Reasonable agreement was obtained between the measured and theoretical end-plate effects of horizontal tails on vertical tails, and the data indicated that the end-plate effect was determined more by the location of the horizontal tail than by the span of the horizontal tail. The horizontal tail gave most end-plate effect when located near either tip of the vertical tail and, when located near the base of the vertical tail, the end-plate effect was increased by moving the horizontal tail rearward.

## INTRODUCTION

A study of the end-plate effect of the horizontal tail on the vertical tail has been made by lifting-line theory for the case of a horizontal tail mounted at the base of an isolated vertical tail (reference 1). A minimum-induced-drag theory of the end-plate effect of the horizontal tail on the vertical tail is presented in reference 2 for the case of a horizontal tail mounted in various vertical locations. Because of a deficiency in experimental data for the end-plate effects discussed

in these references and for end-plate effects in general, the present investigation was undertaken. Lift and hinge-moment measurements were made to determine the variation of the end-plate effect with horizontal-tail span and location and to define an area-span convention that would most nearly give the correct lift-curve slope.

## SYMBOLS

The coefficients and symbols used herein are defined as follows:

| | |
|---|---|
| $C_L$ | lift coefficient $(L/qS)$ |
| $C_h$ | rudder hinge-moment coefficient $\left(H/qb_r(\overline{c_r})^2\right)$ |
| $L$ | lift of model |
| $H$ | rudder hinge moment; positive when moment tends to rotate trailing edge to left |
| $S$ | area of vertical-tail model as defined by convention I (fig. 1) unless otherwise noted |
| $c$ | local chord of vertical-tail model from leading edge (L.E. defined in fig. 1) |
| $\overline{c_r}$ | rudder root-mean-square chord |
| $b_1$ | span (recommended in reference 3) of vertical-tail model as defined by convention I or II, figure 1 |
| $b_2$ | span of vertical-tail model as defined by convention III, figure 1 |
| $b_r$ | rudder span |
| $b_h$ | horizontal tail span |
| $q$ | free-stream dynamic pressure |
| $x$ | horizontal location of 50-percent chord line of forward, center, and rearward end plates as measured from vertical-tail leading edge (L.E. defined in fig. 1) |

$y$ vertical location of end plates measured upward from base of vertical tail as shown in figure 1

$\alpha$ angle of attack of vertical tail; positive when trailing edge is moved to left

$\delta$ rudder deflection relative to fin; positive when trailing edge is deflected to left

$A_G$ geometric aspect ratio

$A$ vertical-tail aspect ratio computed from measured lift for horizontal-tail-off condition

$A_e$ effective aspect ratio computed from measured lift for horizontal-tail-on condition

$E_{e_c}$ effective edge-velocity correction for lift

$k$ horizontal-location factor

Slopes:

$a_o$ section lift-curve slope

$$C_{L_\alpha} = \left(\frac{\partial C_L}{\partial \alpha}\right)_{\delta=0^\circ}$$

$$C_{h_\alpha} = \left(\frac{\partial C_h}{\partial \alpha}\right)_{\delta=0^\circ}$$

$$C_{L_\delta} = \left(\frac{\partial C_L}{\partial \delta}\right)_{\alpha=0^\circ}$$

$$C_{h_\delta} = \left(\frac{\partial C_h}{\partial \delta}\right)_{\alpha=0^\circ}$$

All angles are in degrees and the symbols outside the parentheses indicate the quantities held constant. The slopes were taken for ranges of $\alpha$ and $\delta$ of $\pm 2^\circ$.

## APPARATUS AND MODEL

A vertical-tail model with stub fuselage was tested in combination with horizontal tails simulated by flat

end plates made of $\frac{3}{4}$-inch-thick laminated mahogany with rounded leading edges and beveled trailing edges. Photographs of the model that show variations in the span and location of the end plates are presented as figure 2. The principal details of the model are given in figure 3.

The geometric characteristics of the model are presented in the following table:

| | |
|---|---|
| Area, convention I (fig. 1), square feet | 5.985 |
| Span of vertical-tail model, convention I, feet | 3.61 |
| Mean geometric chord of vertical-tail model, feet | 1.66 |
| Rudder span, feet | 3.208 |
| Rudder root-mean-square chord, feet | 0.646 |
| Trailing-edge angle, vertical tail, degrees | 15 |
| Trailing-edge angle, end plates, degrees | 41 |

The ordinates of the vertical-tail airfoil section are given in table I, the airfoil section being constant over the span. Forward of the 50-percent-chord station the airfoil ordinates are approximately the same as those of the NACA 65(112)-011 airfoil; rearward of the 50-percent-chord station the airfoil was modified so as to eliminate the cusp. The plan-form ordinates of the vertical-tail model are given in table II.

The internal balance for the rudder of the model was contained in four spanwise chambers, which were separated from each other at the rudder hinges. The nose and ends of the internal balance plate in each chamber were sealed to the front of the balance chamber and to the sides of the hinges with Koroseal coated voile. An enlarged cross-sectional diagram of the vertical tail (fig. 4) shows the details of the internal balance.

Unpublished calculations based on reference 4 for an airfoil section approximately the same as that of the model tested indicated that, at a flight Reynolds number of about 10,000,000 and with transition at the leading edge, the boundary-layer thickness $\delta^*$ is 0.00157c at 0.65c. From boundary-layer measurements it was found that, at values of $\alpha$ and $\delta$ of approximately 0°, a boundary-layer thickness of 0.00157c could be obtained by placing roughness strips at the 20-percent chord line. The roughness strips were prepared by cementing

No. 60 carborundum particles in a strip 1/4 inch wide to the back of cellulose tape.

The model was mounted horizontally in the 6- by 6-foot test section of the Langley stability tunnel and was supported entirely by the balance frame so that all forces and moments acting on the model could be measured. In order to mount the model near the center of the tunnel, a model support was used that extended into the air stream through an opening in the tunnel wall. A flexible seal was used between the model support and the tunnel wall to prevent the inward flow of air from outside the tunnel along the model support. A fairing was installed around the part of the model support strut located inside the tunnel. (See fig. 3.) This fairing was attached to the tunnel wall and did not change attitude as the angle of attack of the model was varied.

## TESTS

Tests were made of the vertical-tail model and stub fuselage without an end plate and with an end plate in nine combinations of end-plate locations and spans. A 6-foot-span end plate was tested in the vertical locations designated in figure 5 as low, intermediate-low, intermediate-high, and high. End plates of various spans were tested in the center horizontal location at two vertical locations: A 4-foot-span end plate was tested in the low and in the intermediate-low vertical locations and a 2-foot-span end plate was tested in only the low vertical location. The 6-foot-span end plate in the low vertical location was tested in three horizontal locations, which will be designated as forward, center, and rearward. The configuration for the end plate at the center horizontal location was identical with that at the low vertical location. For all configurations the end plate had a cut-out for the rudder. (See fig. 3.) In order to determine the effect of the rudder cut-out, a 4-foot-span end plate without a cut-out was tested in the low vertical location.

For each configuration, tests were made for various rudder deflections with the model at zero angle of attack and for various angles of attack with zero rudder deflection. The angles of attack ranged from approximately $-4^\circ$ to $16^\circ$, and the rudder deflections, from $-20^\circ$ to $8^\circ$

throughout the tests. The geometric angle of attack of the end plate was maintained at zero. The tests included measurements of the lift of the model and measurements of the rudder hinge moment.

All tests were made at a dynamic pressure of 64.3 pounds per square foot, which corresponds to an airspeed of 159 miles per hour under standard sea-level atmospheric conditions. The Reynolds number based on the mean geometric chord of the vertical tail was approximately 2,400,000.

Jet-boundary corrections, as determined by the general methods described in reference 5, were applied to the lift coefficient, rudder hinge-moment coefficient, and angle of attack. These corrections, which neglected the presence of the end plate, were added directly to the lift and hinge-moment coefficients and to the angle of attack, respectively, and are as follows:

$$\Delta C_L = -0.0102 C_L$$

$$\Delta C_h = 0.0065 C_L$$

$$\Delta \alpha = 0.26 (C_L)_{\delta=0^\circ} + 1.70 C_L$$

No corrections or tares were applied for the effects of the model support-strut fairing or for the effect of the exposed rudder hinge-moment linkage. This linkage may be seen in the photographs of figure 2 and in the sketches of figure 3. An attempt to calculate the effect of the support-strut fairing on the lift of the vertical tail by lifting-line theory was unsuccessful. A rough estimation of this effect based on reference 6 indicated, however, that the support-strut fairing might possibly increase the vertical-tail lift as much as 3.5 percent.

## THEORY

The theory of reference 1, in which the root chords of the horizontal and vertical tails are assumed to coincide and to be the same length accounts for the effect of end-plate span on the effective aspect ratio

of the vertical tail. In this theory, the horizontal tail is assumed to be mounted at the base of the vertical tail. The minimum-induced-drag theory of reference 2 accounts for the vertical location of the end plates on a vertical tail that is symmetrical about both its midspan and midchord lines. The theory of reference 2 also accounts for the end-plate span but assumes the end-plate chord to be infinite. A combination of the results of these two theories is shown in figure 5 in which the results of reference 1 are used to extrapolate those of reference 2 to a finite end-plate chord. In figure 5 the effect of end-plate vertical location is indicated to be much greater than either the effect of end-plate span or vertical-tail aspect ratio and the end plates located near either tip of the vertical tail are shown to have the largest effects. The lift-curve slope for vertical tails with end plates can be estimated by the following formula from lifting-line theory:

$$C_{L_\alpha} = \frac{A\left(A_e/A\right)\pi a_o}{A\left(A_e/A\right)\pi + a_o} \qquad (1)$$

A better result can probably be obtained, however, from the following equation based on lifting-surface theory:

$$C_{L_\alpha} = \frac{A\left(A_e/A\right)\pi a_o}{A\left(A_e/A\right)\pi E_{e_c} + a_o} \qquad (2)$$

where the form of equation (2) is taken from reference 7 and the values of $E_{e_c}$ are taken from reference 8. A chart from which values of $C_{L_\alpha}$ may be conveniently obtained is presented as figure 6.

## RESULTS AND DISCUSSION

Results of the tests are given in figures 7 to 11. The analysis of the data (figs. 12 to 18) was made by a study of the lift and hinge-moment slopes through zero angle of attack and through zero rudder deflection.

## Effect of Vertical Location of End Plate

The variations with $\alpha$ and $\delta$ of lift and rudder hinge-moment coefficients of the vertical tail for various vertical locations of the 6-foot-span end plate in the center horizontal location are presented in figure 7. The greatest end-plate effects, as indicated by the higher values of $C_{L_\alpha}$ and $C_{L_\delta}$, were obtained with the end plate in either the low or high location. (See fig. 12.) As might be expected, the results for the intermediate locations show almost no change from the results for the horizontal-tail-off condition. A determination of the rudder lift-effectiveness parameter $\left(\frac{\alpha}{\delta}\right)_{C_L}$ for the end-plate locations of figure 12 showed this parameter to be constant within the accuracy of the data and to have the value

$$\left(\frac{\alpha}{\delta}\right)_{C_L} = \frac{C_{L_\delta}}{C_{L_\alpha}} = 0.576$$

A curve of the theoretical end-plate effect, obtained by use of figure 5 and equation (2), is also shown in figure 12. Two discrepancies between the theoretical curve and the test points are noticeable. First, because the vertical-tail plan form was not symmetric about its center section, the test points fail to indicate, as does the theory, a zero end-plate effect at the center section of the vertical tail. Second, the end plates near the base of the vertical tail do not produce as much effect as indicated by the theory, although a slightly larger effect would be expected because of the asymmetry of the vertical-tail plan form. This second discrepancy probably results from two factors: The support strut probably causes the end-plate effect to correspond to that of an end plate at a vertical location farther from the base of the vertical tail. Also, the stub fuselage probably had an end-plate effect, for unpublished tests have indicated that a stub fuselage such as the one on this model can have an end-plate effect on $C_{L_\alpha}$ of approximately 5 percent. This increment of end-plate effect would be absorbed by another end plate mounted near the stub fuselage and the resulting effect would be smaller than that expected for an end plate mounted on a model without stub fuselage.

The theoretical curve is believed to be approximately correct when the conditions for which it was derived are met.

The value of $C_{h_\alpha}$ was very close to zero for each of the four vertical locations in which the model was tested. Values of $C_{h_\delta}$ ranged from -0.0017 to -0.0021 (see fig. 15) and were negatively largest for the high and low vertical locations. The small changes in $C_{h_\alpha}$ and $C_{h_\delta}$ indicated in figure 15 probably cannot always be expected, particularly for rudders with little or no balance.

## Effect of Horizontal Location of End Plate

The variations with $\alpha$ and $\delta$ of the lift and rudder hinge-moment coefficients of the vertical tail for various horizontal locations of the 6-foot-span end plate in the low vertical location are presented in figure 8. The center and rearward horizontal locations gave the largest values of $C_{L_\alpha}$ and $C_{L_\delta}$. (See fig. 13.) The values of $C_{h_\alpha}$ were approximately zero and the values of $C_{h_\delta}$ ranged from -0.0021 for the forward and center locations to -0.0030 for the rearward location. (See fig. 15.)

## Effect of Varying Span of End Plate

The variations with $\alpha$ and $\delta$ of the lift and rudder hinge-moment coefficients of the vertical tail for end plates of various spans with the end plate mounted in the center horizontal location for the low and the intermediate-low vertical locations are presented in figures 9 and 10, respectively. The presence of the 2-foot-span end plate increased the values of $C_{L_\alpha}$ and $C_{L_\delta}$ appreciably (see fig. 14), but additional end-plate span caused only a slight increase in these parameters. The hinge-moment parameters $C_{h_\alpha}$ and $C_{h_\delta}$ were almost entirely unaffected by increased span. (See fig. 15.) Because the end plate of 6-foot span reached almost to the tunnel wall, this span was effectively

larger than the actual span tested; but even for this end plate the values of the lift parameters were just slightly higher than those for the 2-foot-span configuration. A comparison of the results shown in figure 14 with those of figures 12 and 13 indicates that changes in end-plate span have only a relatively small effect on $C_{L_\alpha}$ and $C_{L_\delta}$ when the end-plate span is greater than one-half the vertical-tail span and that the end-plate location relative to the vertical tail is the more important of the two variables.

## Effect of Rudder Cut-Out

The effect of the rudder cut-out on the lift and rudder hinge-moment coefficients of the vertical-tail model for the center horizontal location of the 4-foot-span end plate in the low vertical location is shown in figure 11. These data indicate that the only appreciable effect of the rudder cut-out in the end plate was a change of about -0.0007 in $C_{h_\delta}$ at small deflections.

## End-Plate Effect in Terms of Effective Aspect Ratio

In order to make the experimental results of this investigation of the end-plate effects of the horizontal tail on the vertical tail comparable to the theoretical results (fig. 5), the lift-curve-slope results were reduced to the form of the ratio of the effective aspect ratio computed from the measured lift for the end-plate-on condition to the aspect ratio computed from the measured lift for the end-plate-off condition $A_e/A$.

The aspect ratios were computed by means of equations (1) and (2), which are based, respectively, on the lifting-line and lifting-surface theory for an isolated wing. The section lift-curve slope $a_o$ was estimated to have a value of 0.105 for the vertical tail. The ratio $A_e/A$ is shown in figure 16 as determined by the lifting-surface theory for all model configurations for area-span convention I of figure 1. With the end plate in the low vertical location, this same ratio $(A_e/A)$ is shown in figure 17 as determined by the lifting-line theory for all three area-span conventions of figure 1. The ratio $A_e/A$ is shown in figures 16 and 17 to depend

only slightly on which formula or which area-span convention is used. The values of $A_e/A$ determined from the test data are shown in figure 17 to be smaller than those from figure 5. This discrepancy is the same as that discussed in connection with the effect of the vertical location of the end plate.

## Estimation of $C_{L_\alpha}$ for a Vertical Tail

If an estimate of $C_{L_\alpha}$ for a vertical tail is desired, an aspect ratio must be arrived at by means of some area-span convention. In the following table a comparison is presented of the geometric aspect ratios and the aspect ratios for the horizontal-tail-off condition as computed by use of equations (1) and (2) for the three area-span conventions shown in figure 1.

| Area-span convention (See fig. 1.) | $A_G$ | A (Equation (1)) | A (Equation (2)) | Corrected A (Equation (2)) |
|---|---|---|---|---|
| I | 2.17 | 1.99 | 2.85 | 2.60 |
| II | 2.05 | 1.77 | 2.58 | 2.38 |
| III | 2.25 | 1.46 | 2.20 | 2.05 |

The corrected values of the aspect ratio were obtained by reducing the lift-curve slope 5 percent to correct the data approximately to the conditions for the model without stub fuselage. The values in the first three columns of aspect ratio indicate that for this model, in order to estimate $C_{L_\alpha}$ for the end-plate-off condition from a geometric aspect ratio, the formula for the lift-curve slope based on lifting-surface theory (equation (2)) should be used in conjunction with area-span convention III. The measured lift-curve slope, however, is probably higher than that which would be realized in flight because of the effect of aerodynamic induction on the support-strut fairing and because of the absence of most of the fuselage sidewash. If data on fuselage sidewash are unavailable, an area-span convention defining the vertical-tail area as that above the fuselage

center line (convention II, fig. 1), as proposed by Pass in reference 3, and corresponding to a somewhat lower lift-curve slope than convention III may more nearly represent the case of the vertical tail on an airplane. In order to estimate $C_{L_\alpha}$ for a vertical tail with the horizontal tail on, use may be made of the effective aspect ratio obtained by multiplying the geometric aspect ratio by $A_e/A$ as given in figure 5.

An average value of $\frac{A_e}{A} = 1.5$ was suggested in reference 3. This value is considerably more than will generally result because it is based on a vertical-tail aspect ratio of 1.4, which is somewhat smaller than the aspect ratios now generally used and, more important, is based on an end plate located at the base of the vertical tail - a condition seldom if ever met in practice.

For tail configurations similar to the 6-foot-span end plate in low vertical location, the effect of horizontal location can be considered by multiplying the value of $A_e/A$ given in figure 5 by the horizontal-location factor $k$ shown in figure 18 and derived from the $C_{L_\alpha}$-data of figure 13.

## CONCLUSIONS

Tests were made of a vertical-tail model with stub fuselage in combination with various simulated horizontal tails to determine the effect of horizontal-tail span and location on the aerodynamic characteristics of the vertical tail, and the test results were compared with theoretical results. The results of the investigation indicated the following conclusions:

1. The theoretical end-plate effect is approximately correct when the conditions for which it was derived are met.

2. The end-plate effect of the horizontal tail on the vertical tail was influenced more by the location of the horizontal tail than by the horizontal tail span.

3. The greatest end-plate effect was obtained with the horizontal tail located near either tip of the vertical tail.

4. When the horizontal tail was located near the base of the vertical tail, the end-plate effect was increased by moving the horizontal tail rearward.

Langley Memorial Aeronautical Laboratory
National Advisory Committee for Aeronautics
Langley Field, Va., January 21, 1946

## REFERENCES

1. Katzoff, S., and Mutterperl, William: The End-Plate Effect of a Horizontal-Tail Surface on a Vertical-Tail Surface. NACA TN No. 797, 1941.

2. Rotta, J.: Luftkräfte am Tragflügel mit einer seitlichen Scheibe. Ing.-Archiv, Bd. XIII, Heft 3, June 1942, pp. 119-131.

3. Pass, H. R.: Analysis of Wind-Tunnel Data on Directional Stability and Control. NACA TN No. 775, 1940.

4. von Doenhoff, Albert E., and Tetervin, Neal: Determination of General Relations for the Behavior of Turbulent Boundary Layers. NACA ACR No. 3G13, 1943.

5. Swanson, Robert S., and Toll, Thomas A.: Jet-Boundary Corrections for Reflection-Plane Models in Rectangular Wind Tunnels. NACA ARR No. 3E22, 1943.

6. Schrenk, O.: A Simple Approximation Method for Obtaining the Spanwise Lift Distribution. NACA TM No. 948, 1940.

7. Jones, Robert T.: Correction of the Lifting-Line Theory for the Effect of the Chord. NACA TN No. 817, 1941.

8. Swanson, Robert S., and Priddy, E. LaVerne: Lifting-Surface-Theory Values of the Damping in Roll and of the Parameter Used in Estimating Aileron Stick Forces. NACA ARR No. L5F23, 1945.

TABLE I

ORDINATES OF VERTICAL-TAIL AIRFOIL SECTION

[Stations and ordinates in percent of airfoil chord]

| Upper surface | | Lower surface | |
|---|---|---|---|
| Station | Ordinate | Station | Ordinate |
| 0 | 0 | 0 | 0 |
| .5 | .845 | .5 | -.845 |
| .75 | 1.019 | .75 | -1.019 |
| 1.25 | 1.270 | 1.25 | -1.270 |
| 2.5 | 1.719 | 2.5 | -1.719 |
| 5 | 2.389 | 5 | -2.389 |
| 7.5 | 2.909 | 7.5 | -2.909 |
| 10 | 3.343 | 10 | -3.343 |
| 15 | 4.036 | 15 | -4.036 |
| 20 | 4.561 | 20 | -4.561 |
| 25 | 4.951 | 25 | -4.951 |
| 30 | 5.242 | 30 | -5.242 |
| 35 | 5.419 | 35 | -5.419 |
| 40 | 5.498 | 40 | -5.498 |
| 45 | 5.454 | 45 | -5.454 |
| 50 | 5.276 | 50 | -5.276 |
| 55 | 4.995 | 55 | -4.995 |
| 60 | 4.622 | 60 | -4.622 |
| 65 | 4.158 | 65 | -4.158 |
| 70 | 3.638 | 70 | -3.638 |
| 75 | 3.087 | 75 | -3.087 |
| 80 | 2.489 | 80 | -2.489 |
| 85 | 1.886 | 85 | -1.886 |
| 90 | 1.279 | 90 | -1.279 |
| 95 | .646 | 95 | -.646 |
| 100 | .030 | 100 | -.030 |

TABLE II

PLAN-FORM ORDINATES OF VERTICAL-TAIL MODEL

[Stations and ordinates are in inches]

| Station (a) | Ordinate (Forward of rudder hinge axis) | Station (a) | Ordinate (Rearward of rudder hinge axis) |
|---|---|---|---|
| -4.500 | ---------- | -4.500 | 0 |
| -4.167 | ---------- | -4.167 | 1.212 |
| -3.667 | ---------- | -3.667 | 2.733 |
| -2.833 | ---------- | -2.833 | 4.294 |
| -2.00 | ---------- | -2.00 | 5.368 |
| -1.167 | ---------- | -1.167 | 6.192 |
| 0 | 17.333 | 0 | 7.067 |
| 1.833 | ---------- | 1.833 | 8.021 |
| 2.167 | ---------- | 2.167 | 8.153 |
| 4.617 | 17.267 | 4.617 | ---------- |
| 5.500 | ---------- | 5.500 | 8.982 |
| 7.167 | ---------- | 7.167 | 9.133 |
| 8.000 | ---------- | 8.000 | 9.155 |
| 9.167 | 16.962 | 9.167 | 9.133 |
| 10.333 | ---------- | 10.333 | 9.078 |
| 12.500 | 16.636 | 12.500 | ---------- |
| 16.667 | 16.072 | 16.667 | 8.654 |
| 20.833 | 15.317 | 20.833 | ---------- |
| 25.000 | 14.340 | 25.000 | 7.721 |
| 29.167 | 13.091 | 29.167 | 7.049 |
| 33.333 | 11.483 | 33.333 | 6.183 |
| 37.500 | 9.332 | 37.500 | 5.025 |
| 39.333 | 8.107 | 39.333 | 4.365 |
| 40.000 | 7.589 | 40.000 | 4.070 |
| 41.667 | 5.944 | 41.667 | 2.913 |
| 42.500 | 4.733 | 42.500 | 1.850 |
| 42.833 | 4.059 | 42.833 | 1.183 |
| 43.000 | 3.629 | 43.000 | .721 |
| 43.167 | 3.062 | 43.167 | .082 |
| 43.333 | 1.667 | 43.333 | -1.667 |

[a]Measured from fuselage center line.

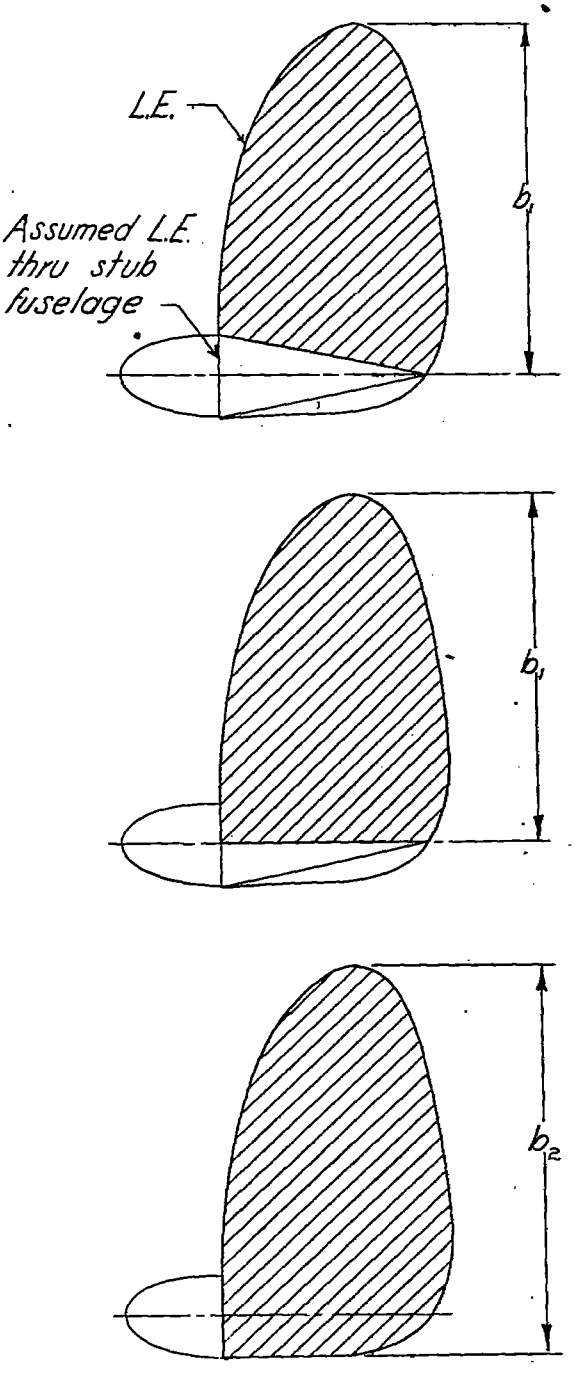


Figure 1.- Three area-span conventions which are used in calculating the aspect ratio and the force and moment coefficients of vertical tails. (Convention II is that recommended in reference 3.)

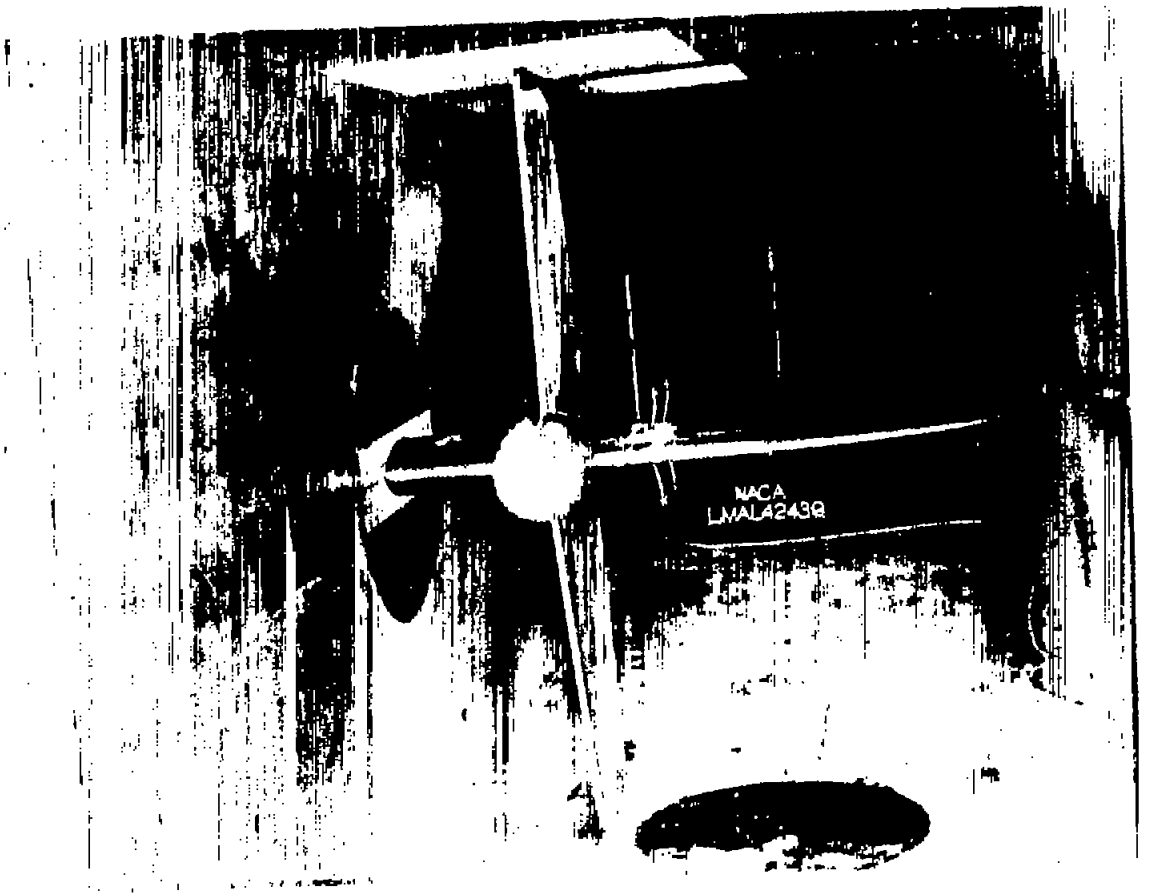


(a) Center horizontal location of the 6-foot-span end plate in low vertical location.

Figure 2.- Front views of the vertical-tail model as mounted in the 6- by 6-foot section of the Langley stability tunnel.

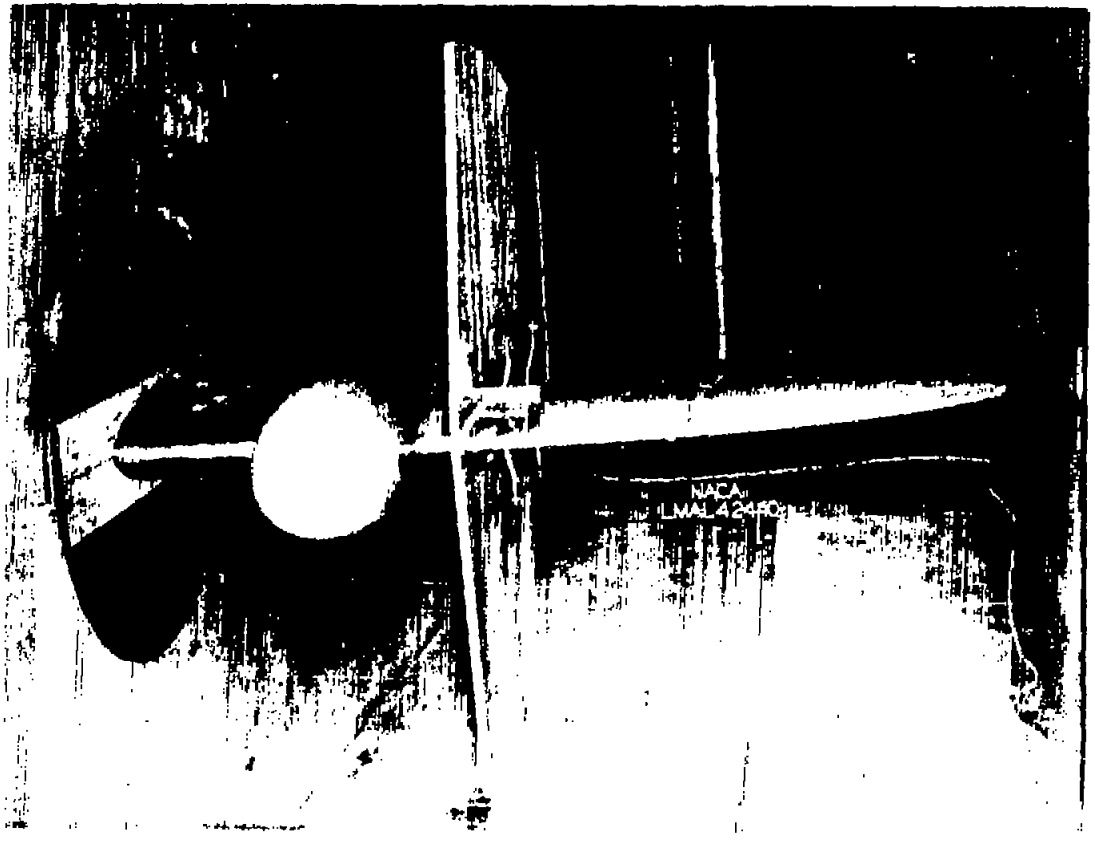


(b) Center horizontal location of the 4-foot-span end plate in the intermediate-low vertical location.

Figure 2.- Concluded.

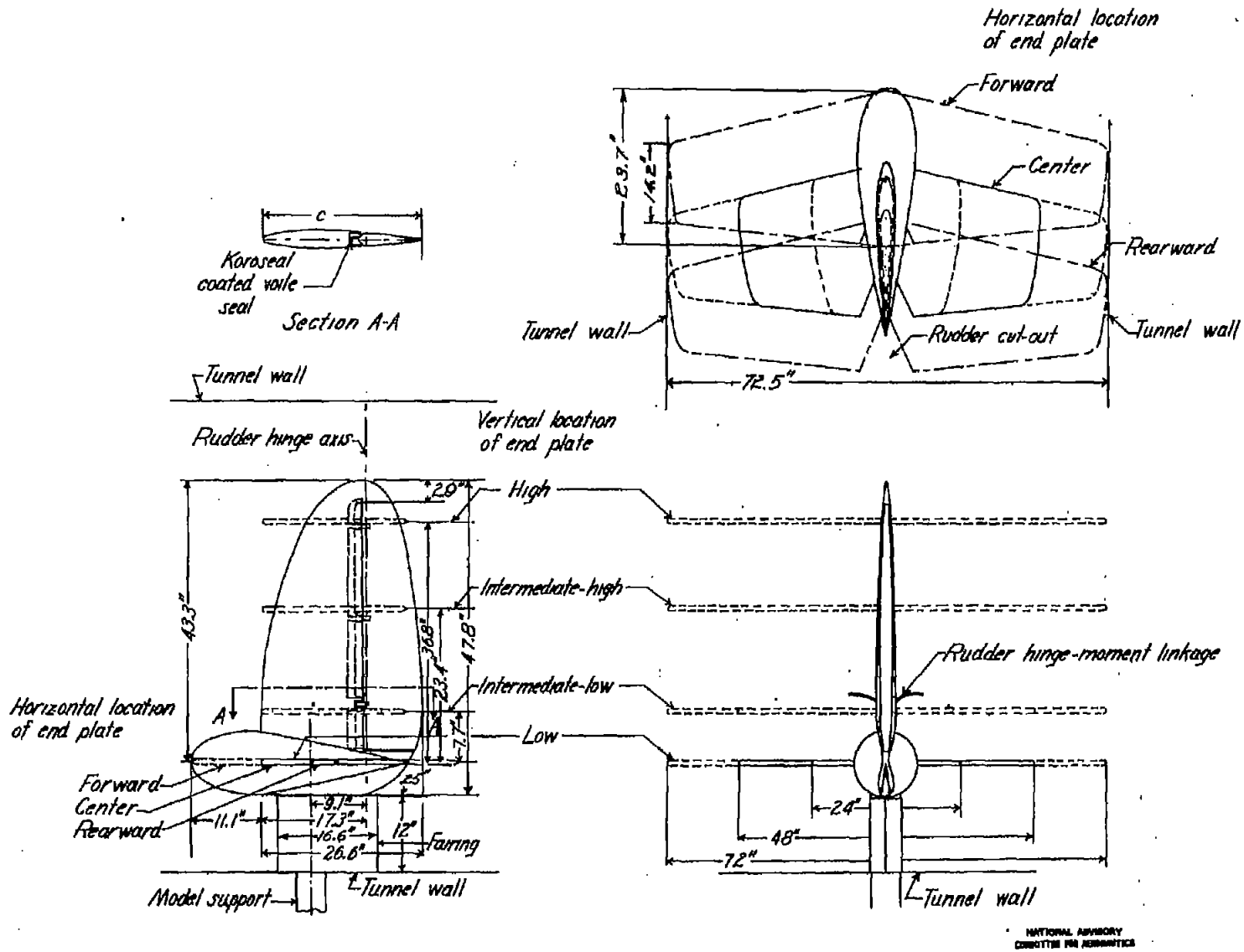


Figure 3.- Details of the vertical-tail model.

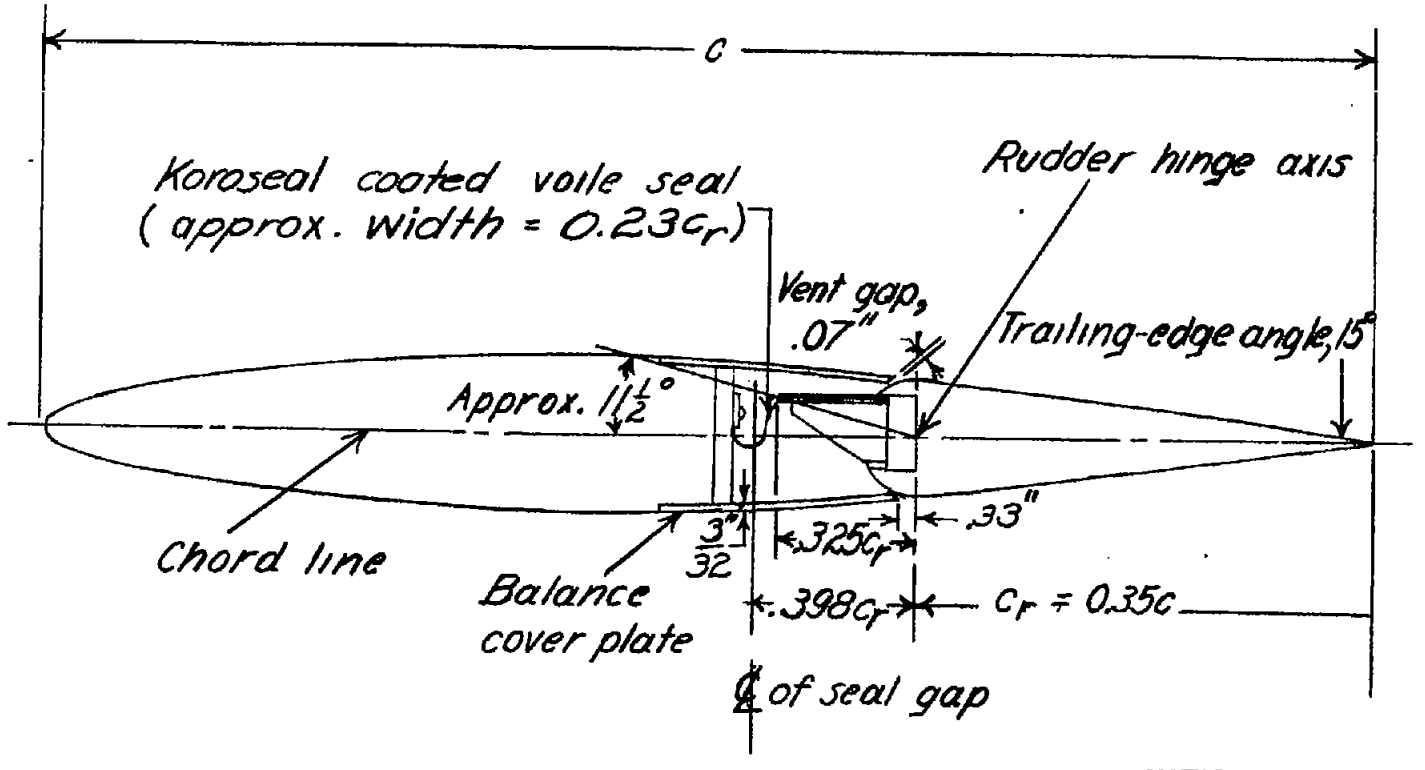


NATIONAL ADVISORY
COMMITTEE FOR AERONAUTICS

Figure 4.-Enlarged cross-sectional diagram of the vertical tail showing details of the internal balance. Rudder movement, 28° right, 8° left.

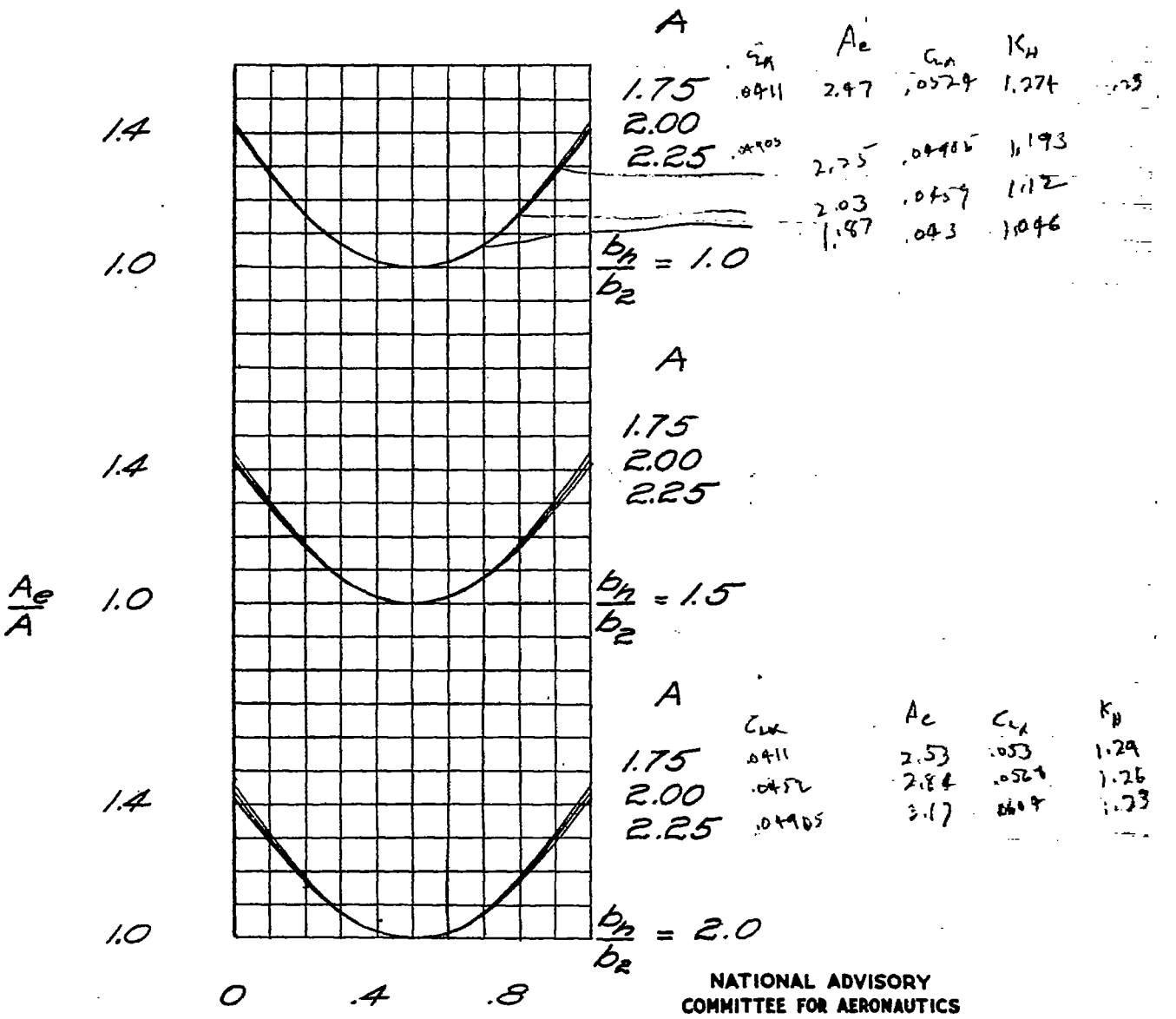


Vertical location of end plate, $\frac{y}{b_2}$

Figure 5.- Effect of end-plate location and span and vertical-tail aspect ratio on the effective-aspect-ratio parameter.

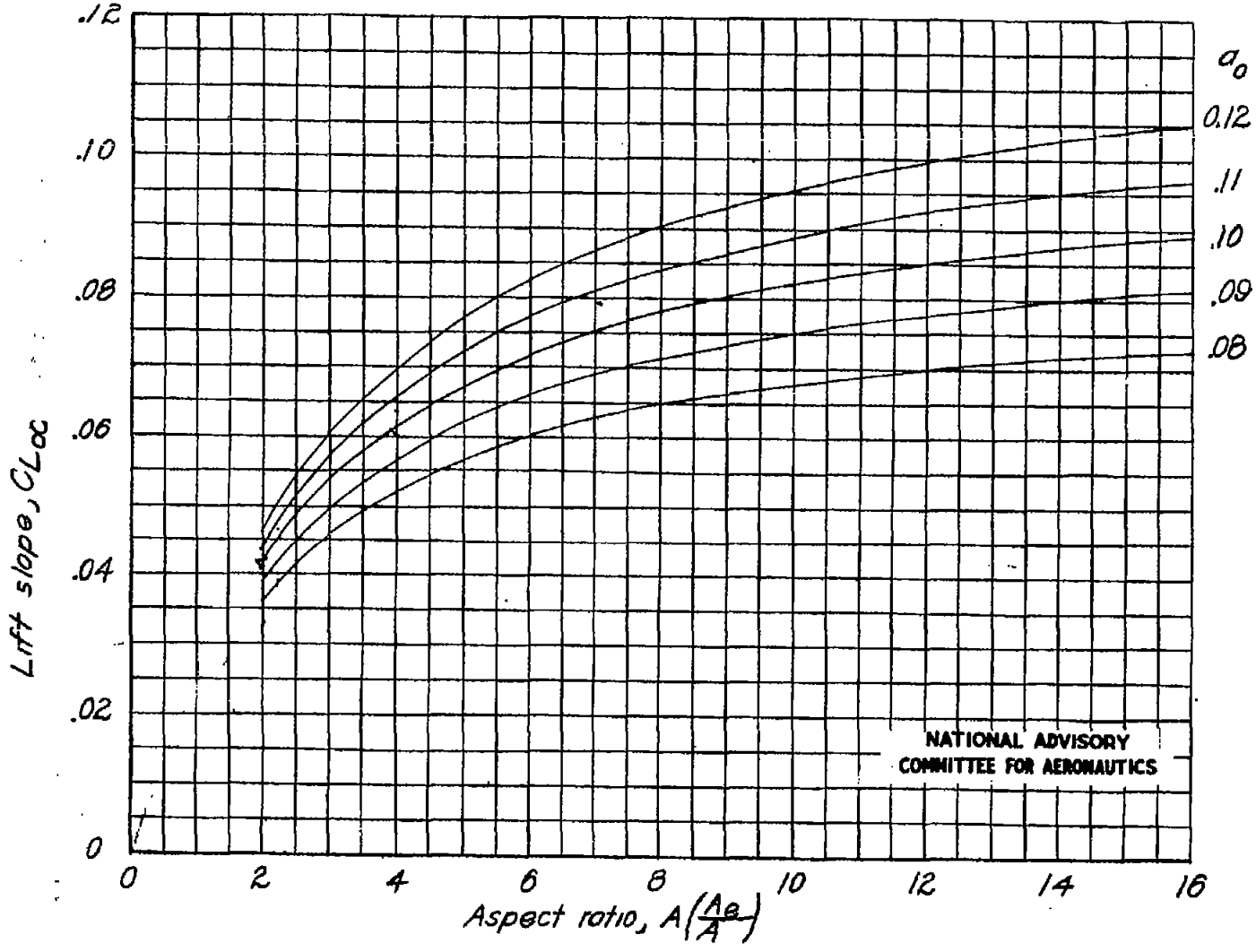


Figure 6.- Chart based on lifting-surface theory for determination of the slope of the lift curve for angles of attack.

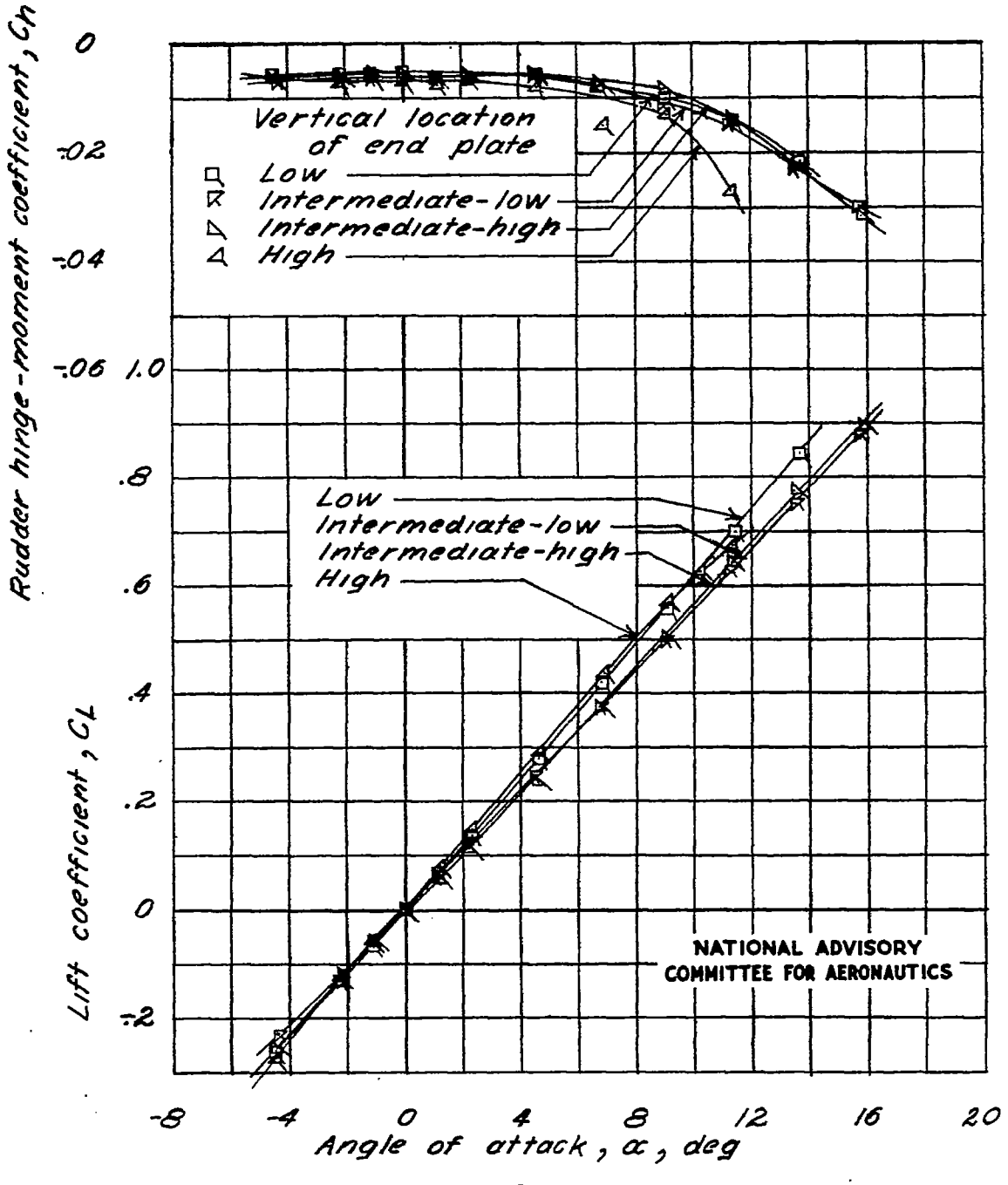


(a) $\delta = 0°$.

Figure 7.- Effect of vertical location of the 6-foot-span end plate in center horizontal location on the lift and rudder hinge-moment characteristics of the vertical-tail model.

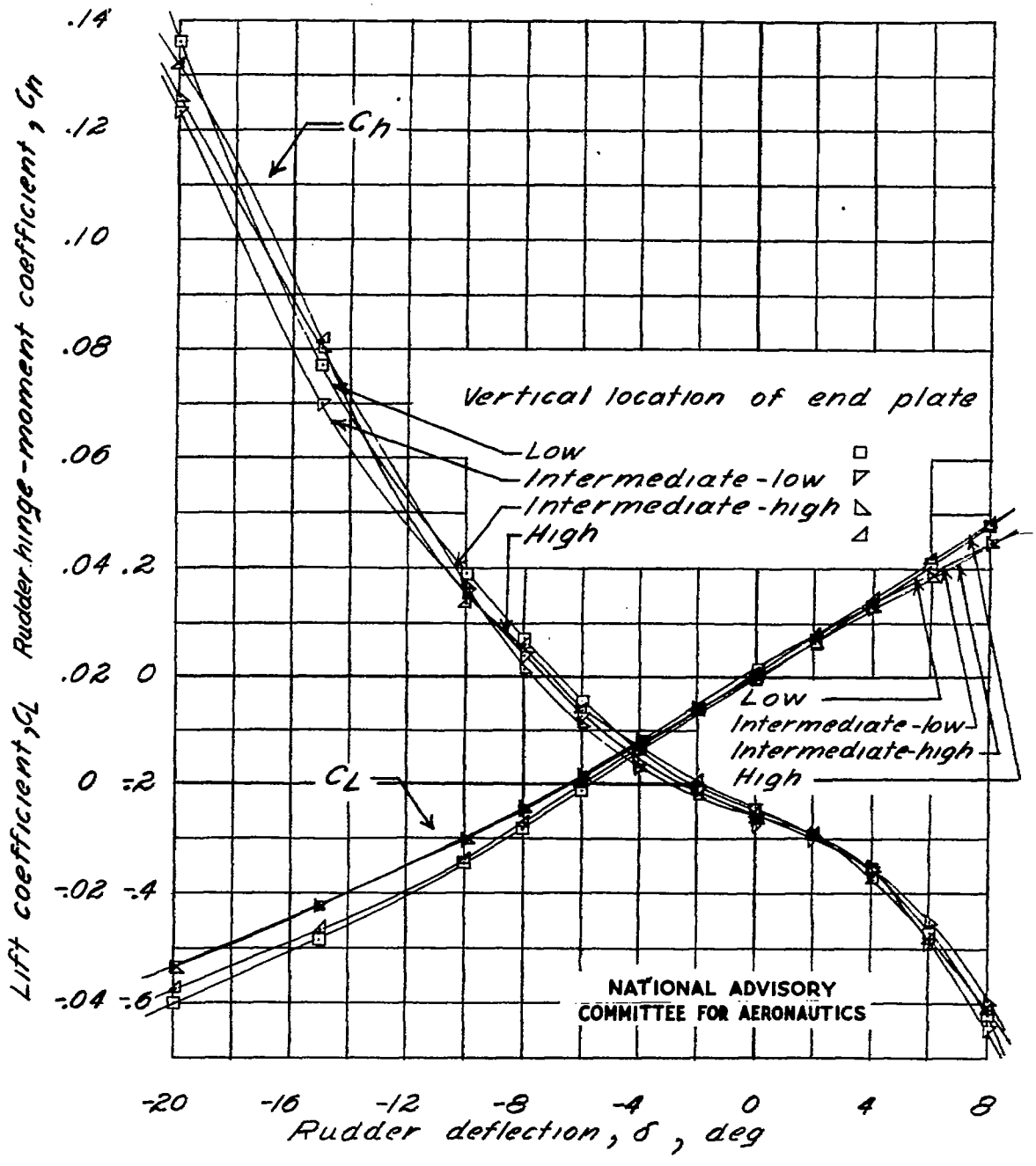


(b) $\alpha = 1.7 C_L$.

Figure 7.- Concluded.

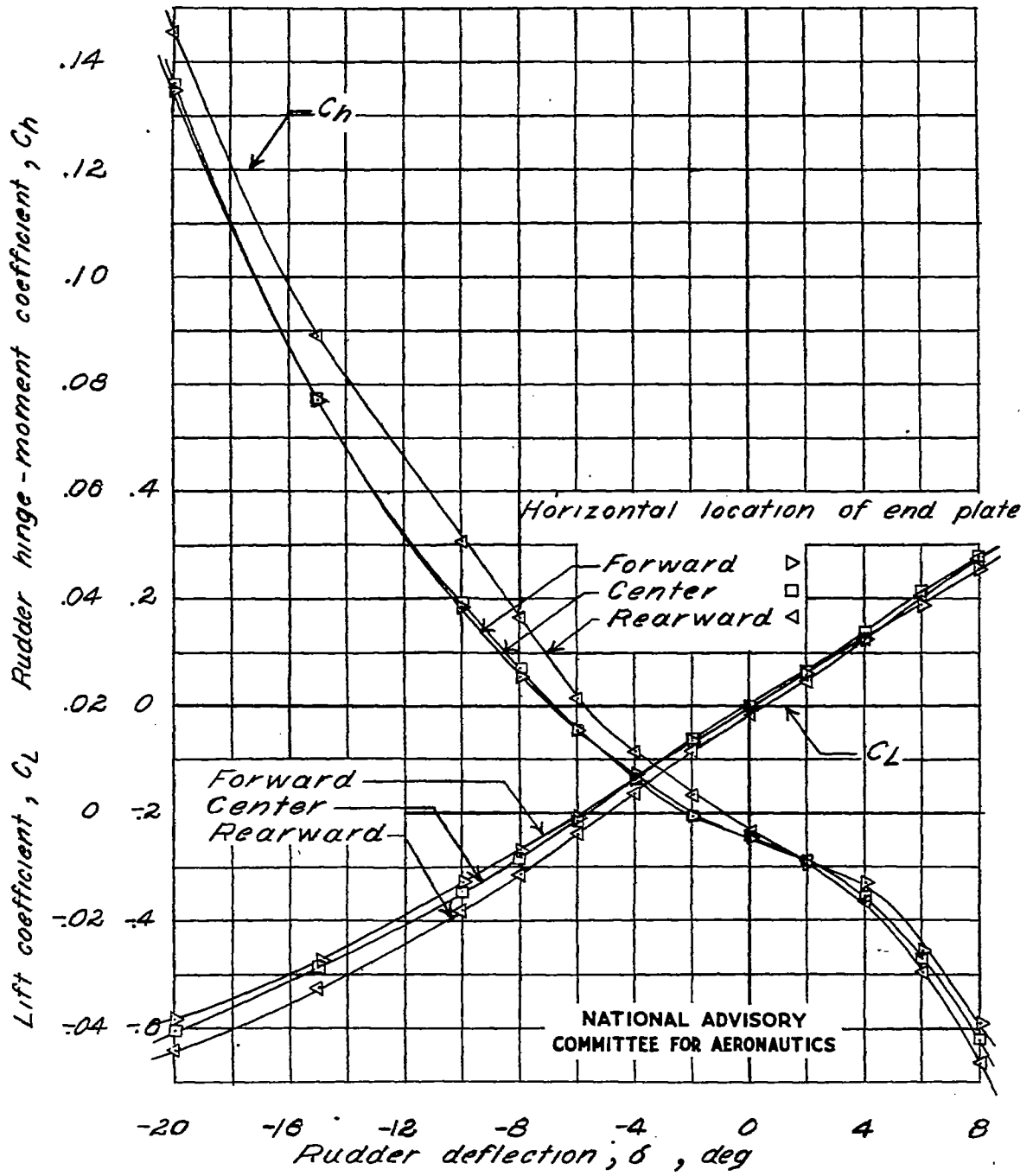


(b) $\alpha = 1.7\,C_L$.

Figure 8.- Concluded.

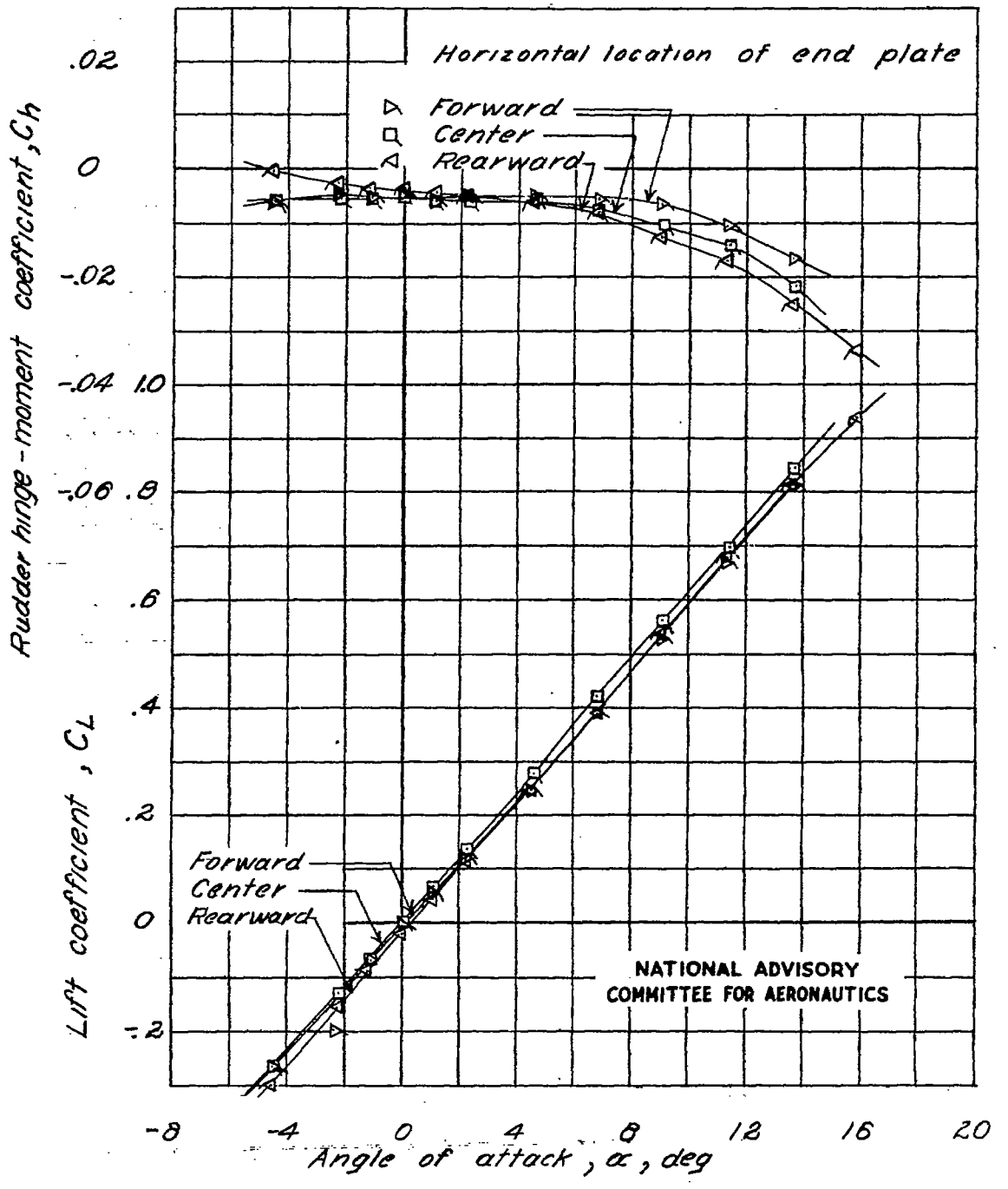


(a) $\delta = 0°$.

Figure 8.-Effect of horizontal location of the 6-foot-span end plate in low vertical location on the lift and rudder hinge-moment characteristics of the vertical-tail model.

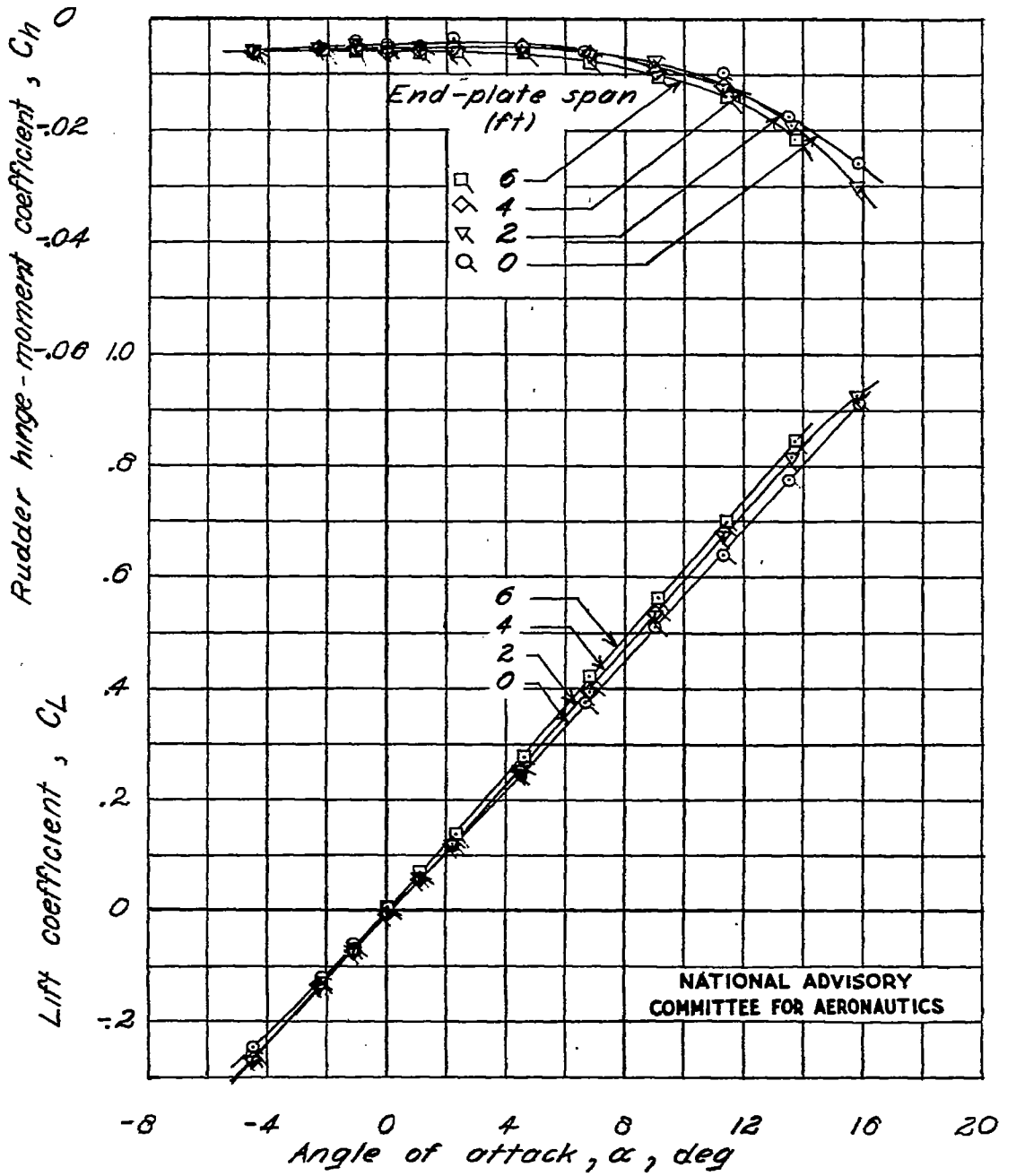


(a) $\delta = 0°$.

Figure 9.- Effect of various end-plate spans in the center horizontal location for the low vertical location on the lift and rudder hinge-moment characteristics of the vertical-tail model.

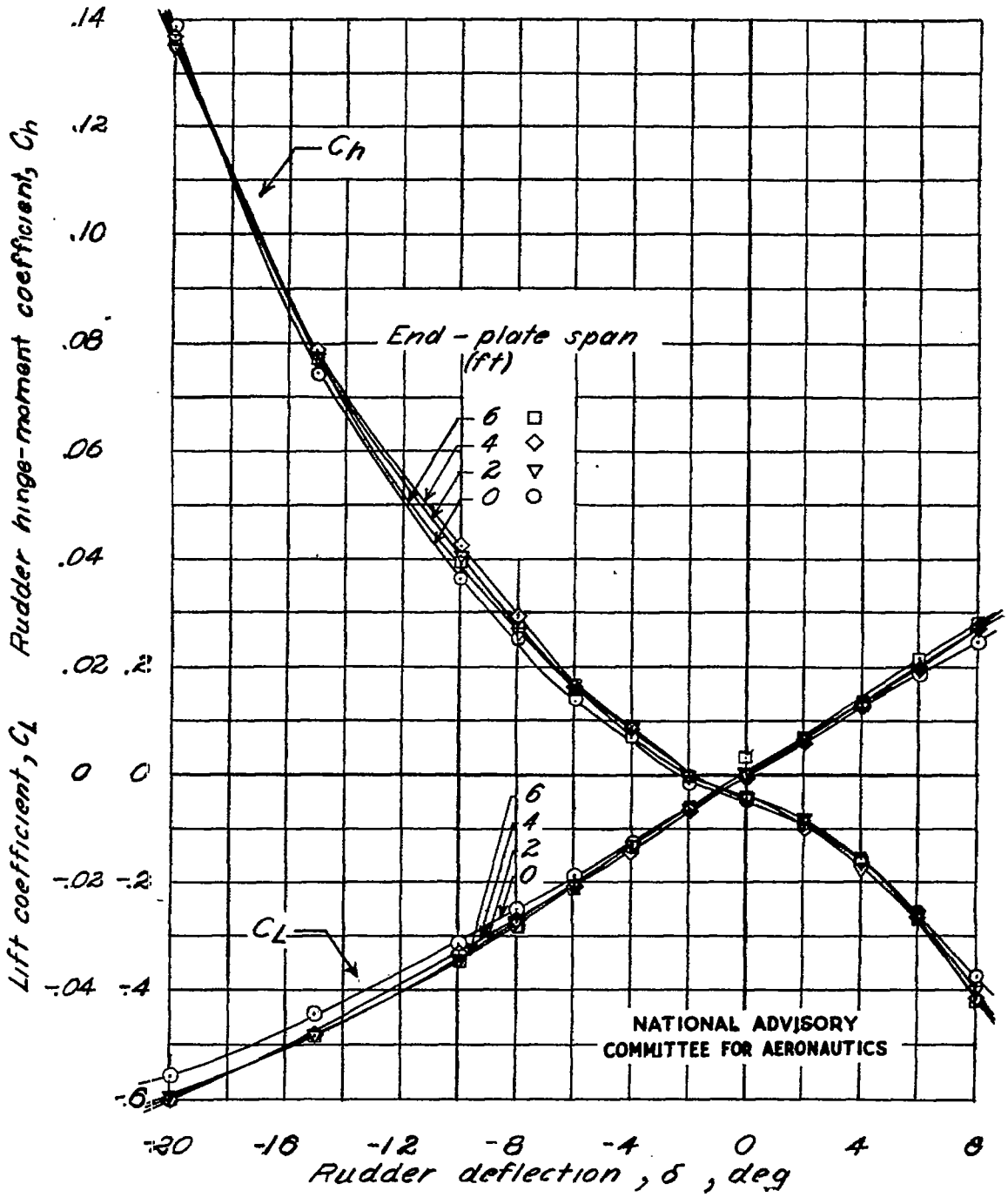


(b) $\alpha = 1.7\ C_L$.

Figure 9.- Concluded.

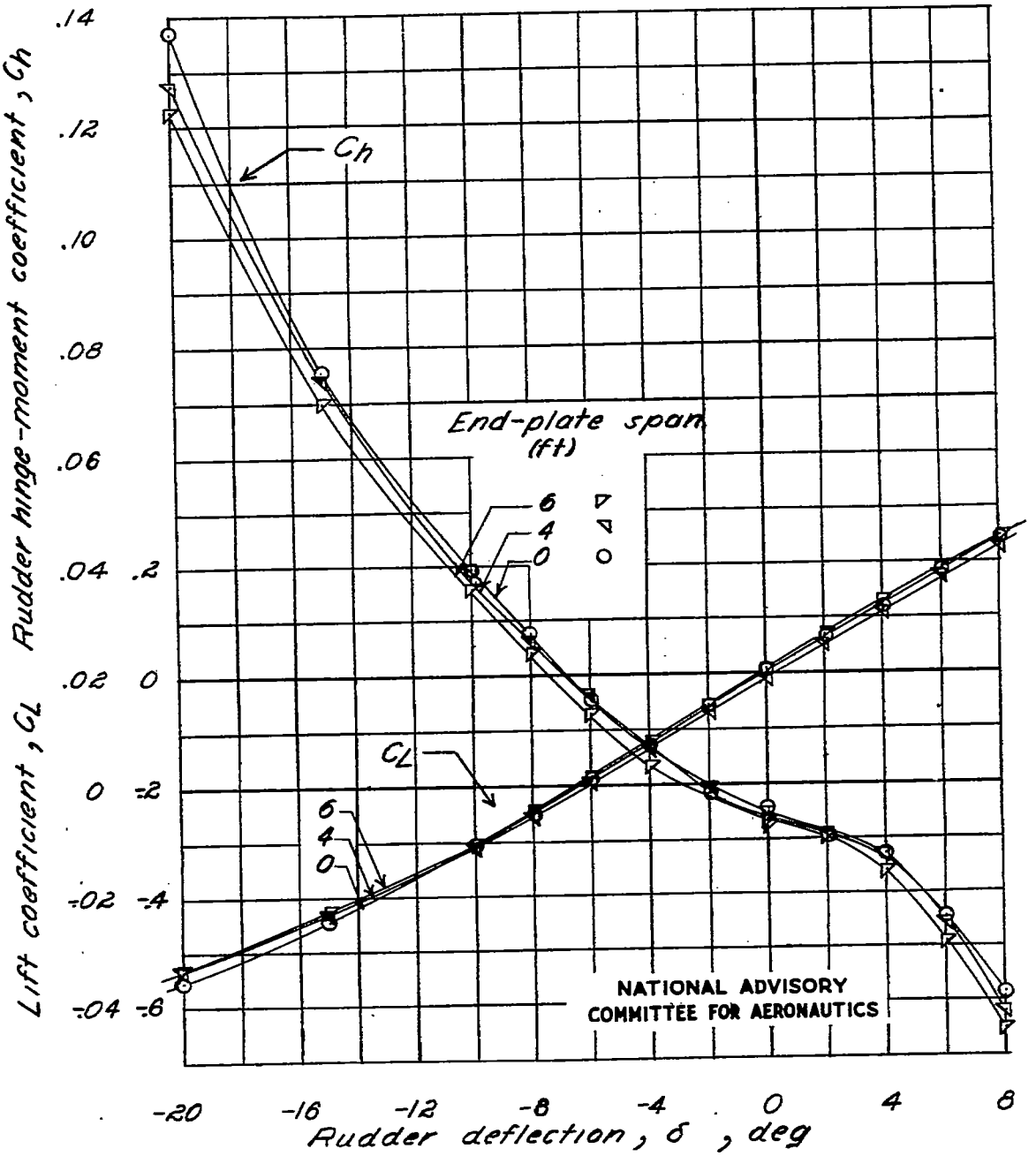


(b) $\alpha = 1.7 C_L$.

Figure 10.--Concluded.

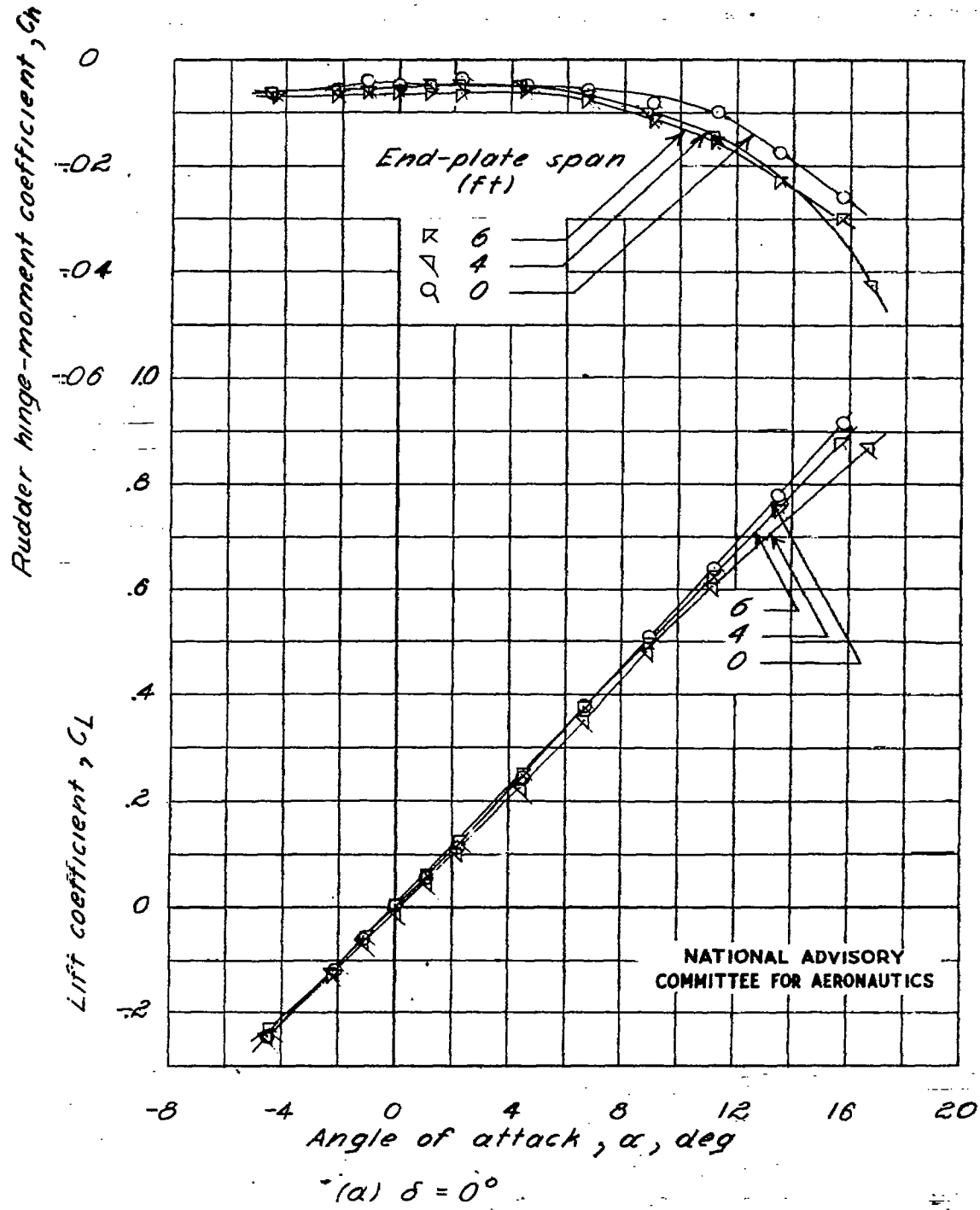


Figure 10.- Effect of various end-plate spans in the center horizontal location for the intermediate-low vertical location on the lift and rudder hinge-moment characteristics of the vertical-tail model.

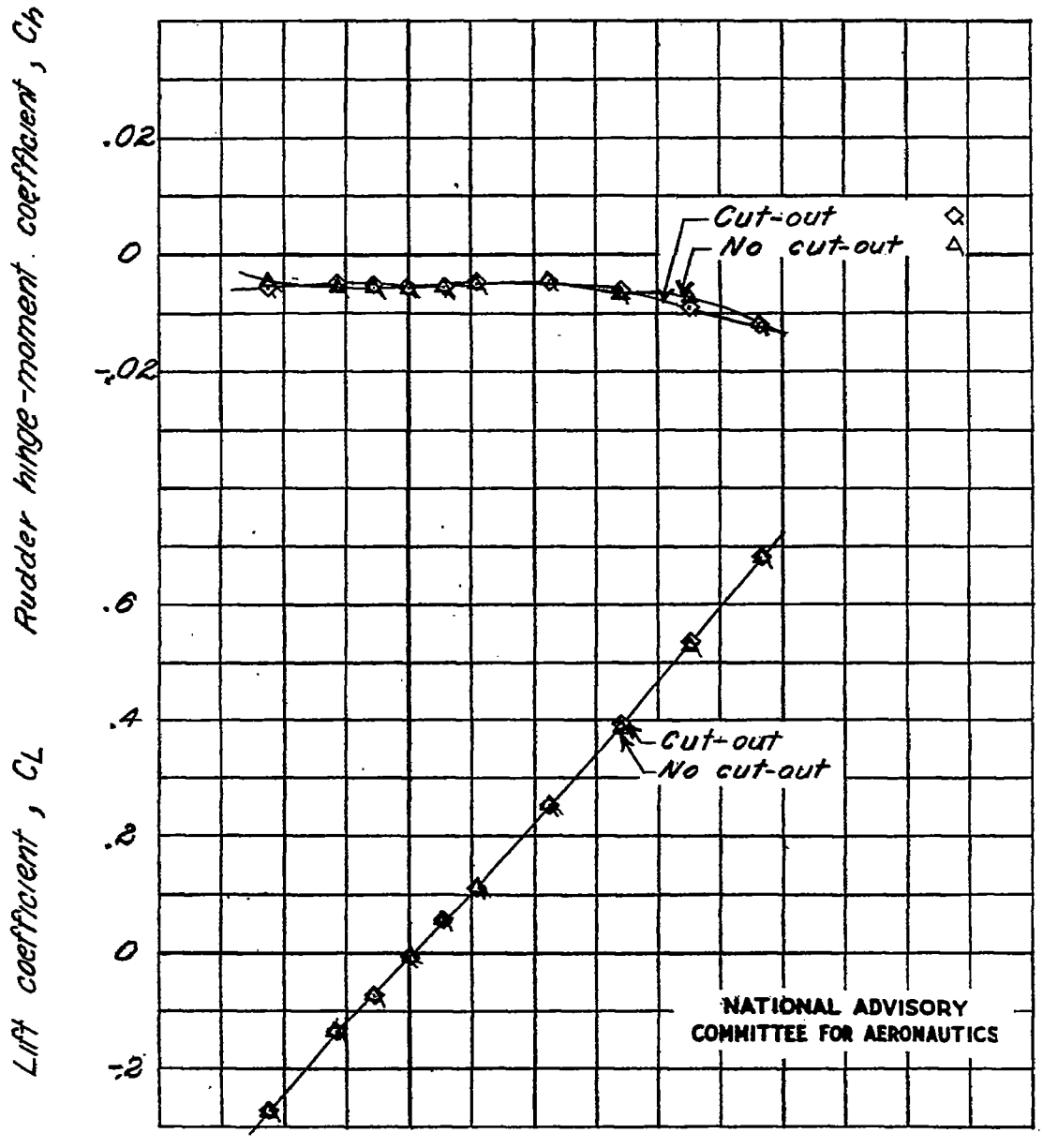


(a) $\delta = 0°$.

Figure 11.-Effect of rudder cut-out on the lift and rudder hinge-moment characteristics of the vertical-tail model for the center horizontal location of the 4-foot-span end plate in low vertical location.

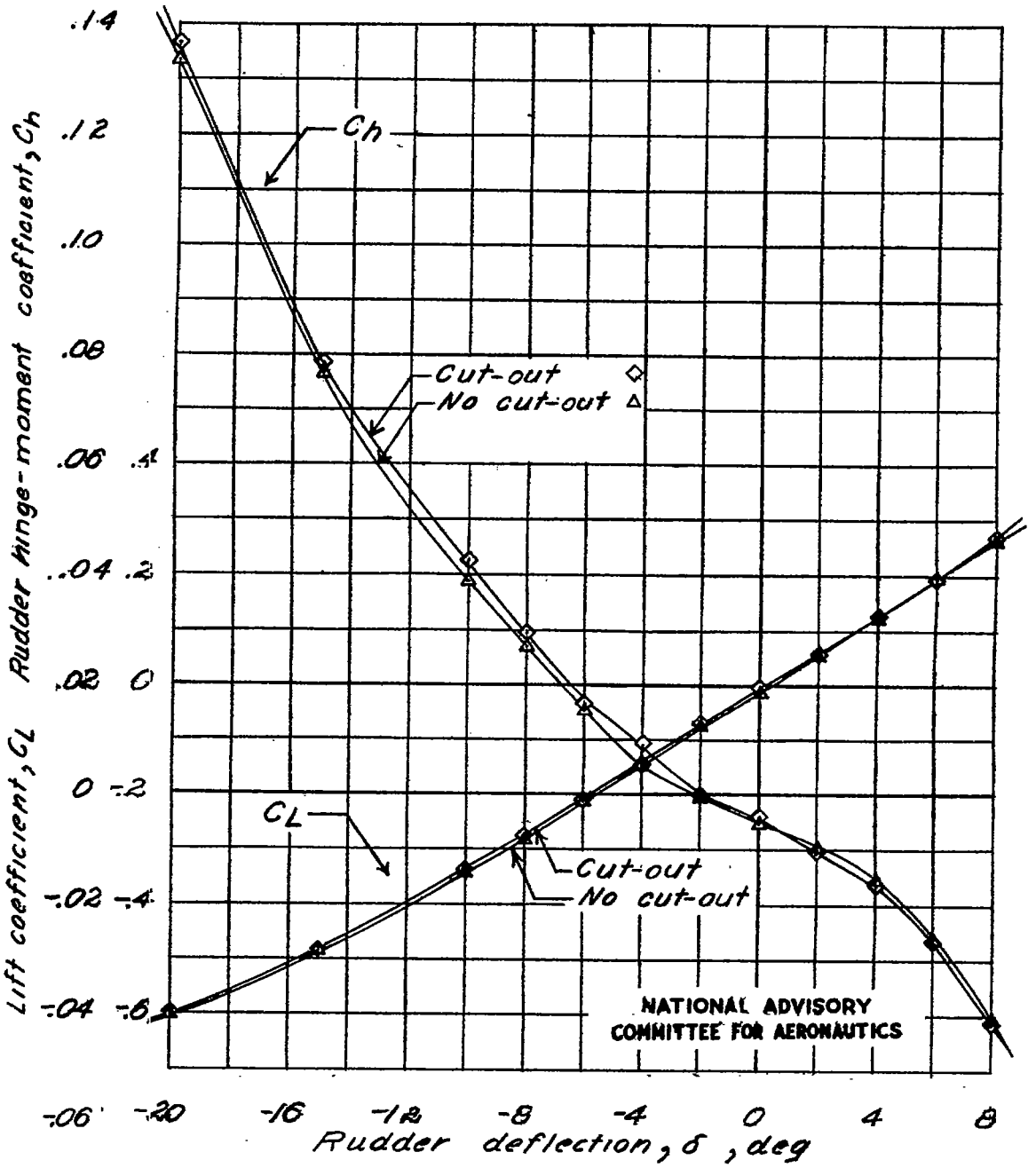


(b) $\alpha = 1.7\,C_L$

Figure 11.- Concluded.

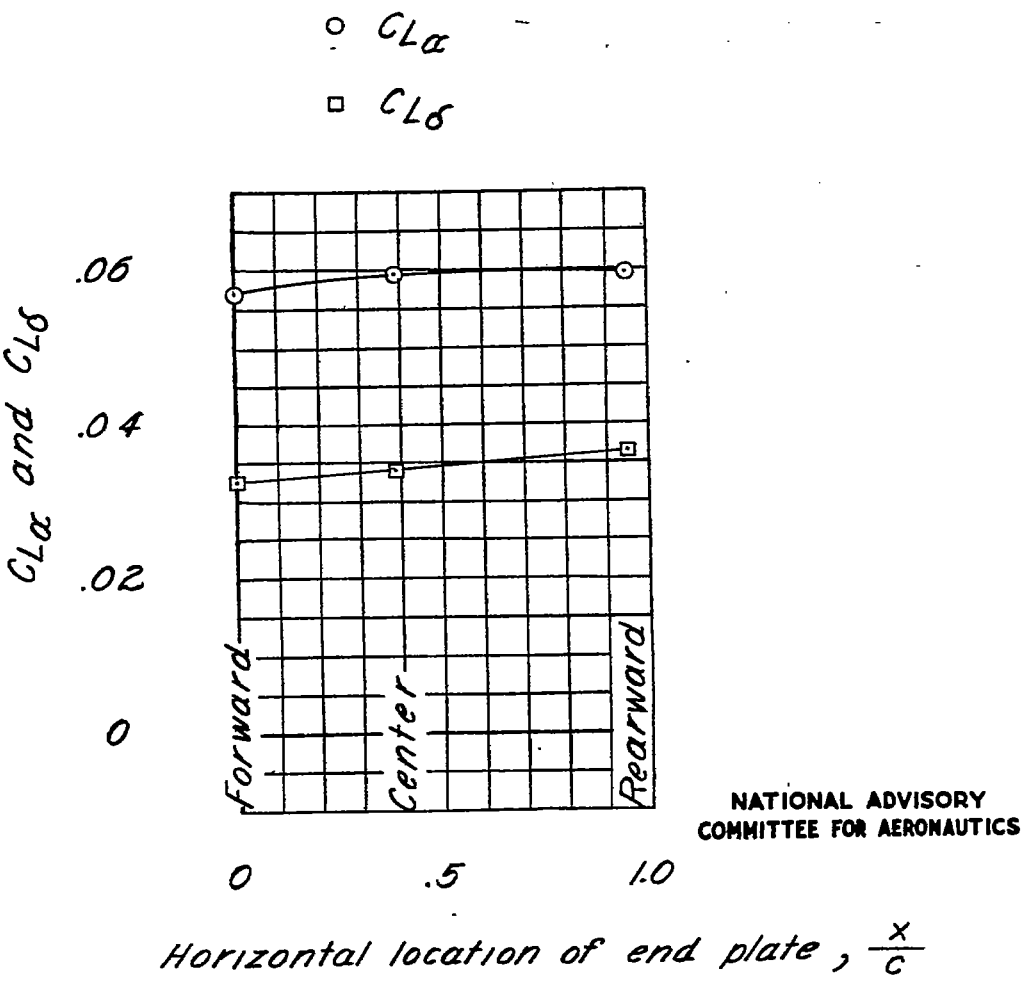


Figure 13.- Effect of horizontal location of a 6-foot-span low end plate on the lift parameters of the vertical-tail model.

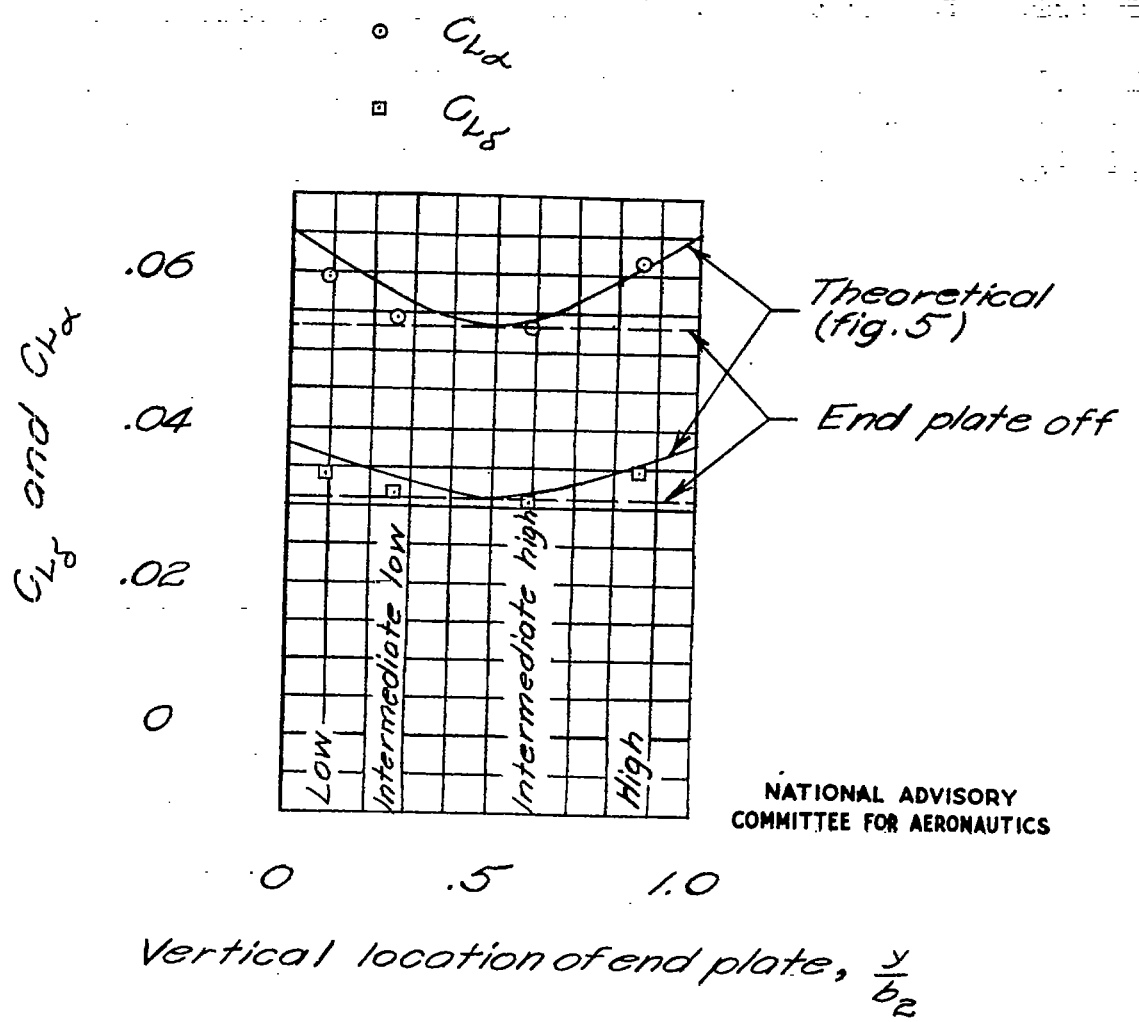


Figure 12.- Effect of vertical location of a 6-foot-span center end plate on the lift parameters of the vertical-tail model.

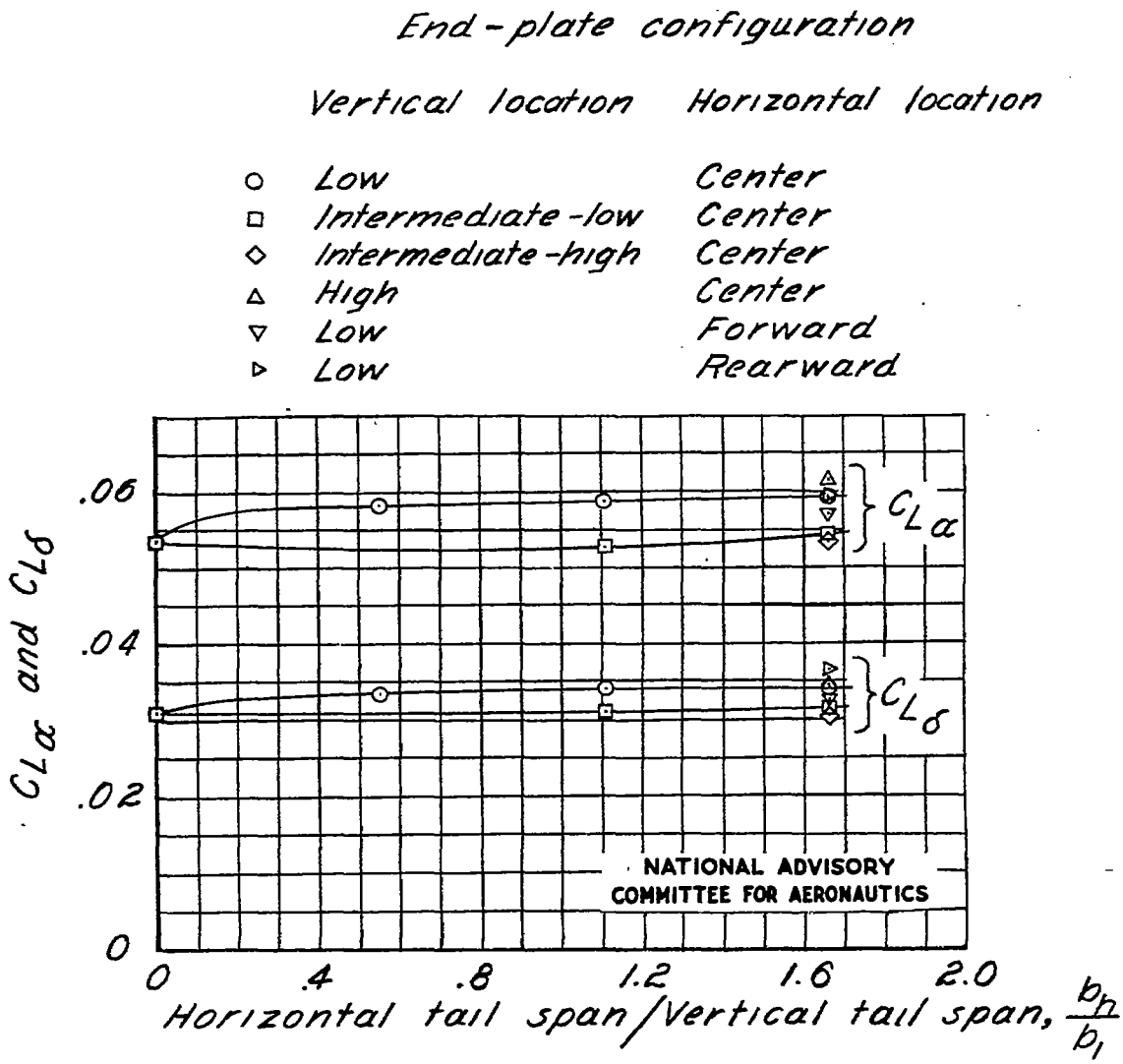


Figure 14.- Effect of end-plate span on the lift parameters of the vertical-tail model.

End-plate configuration

| | Vertical location | Horizontal location |
|---|---|---|
| ○ | Low | Center |
| □ | Intermediate-low | Center |
| ◇ | Intermediate-high | Center |
| △ | High | Center |
| ▽ | Low | Forward |
| ▷ | Low | Rearward |

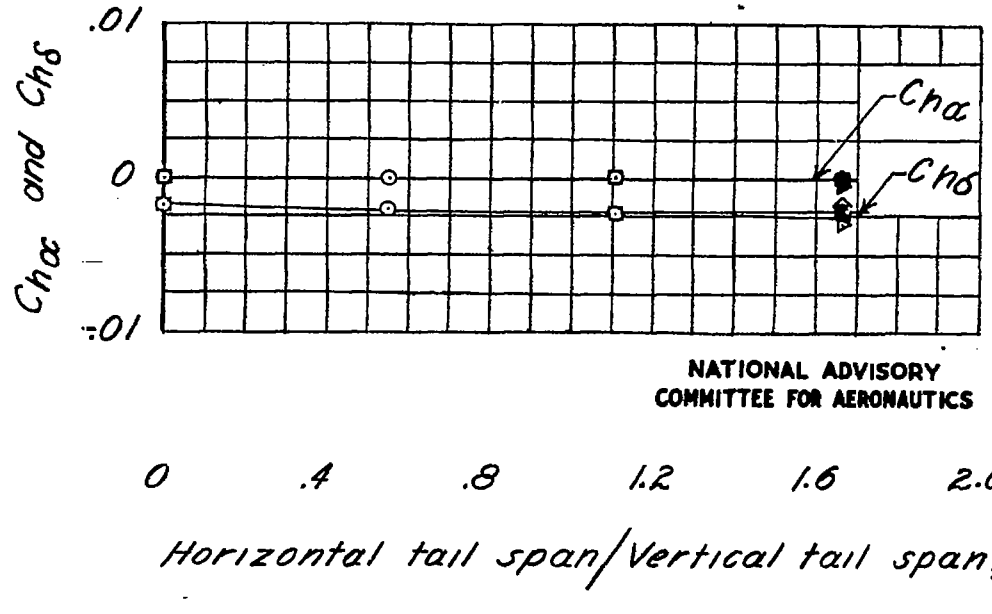


Figure 15.-Effect of end-plate span on the rudder hinge-moment parameters.

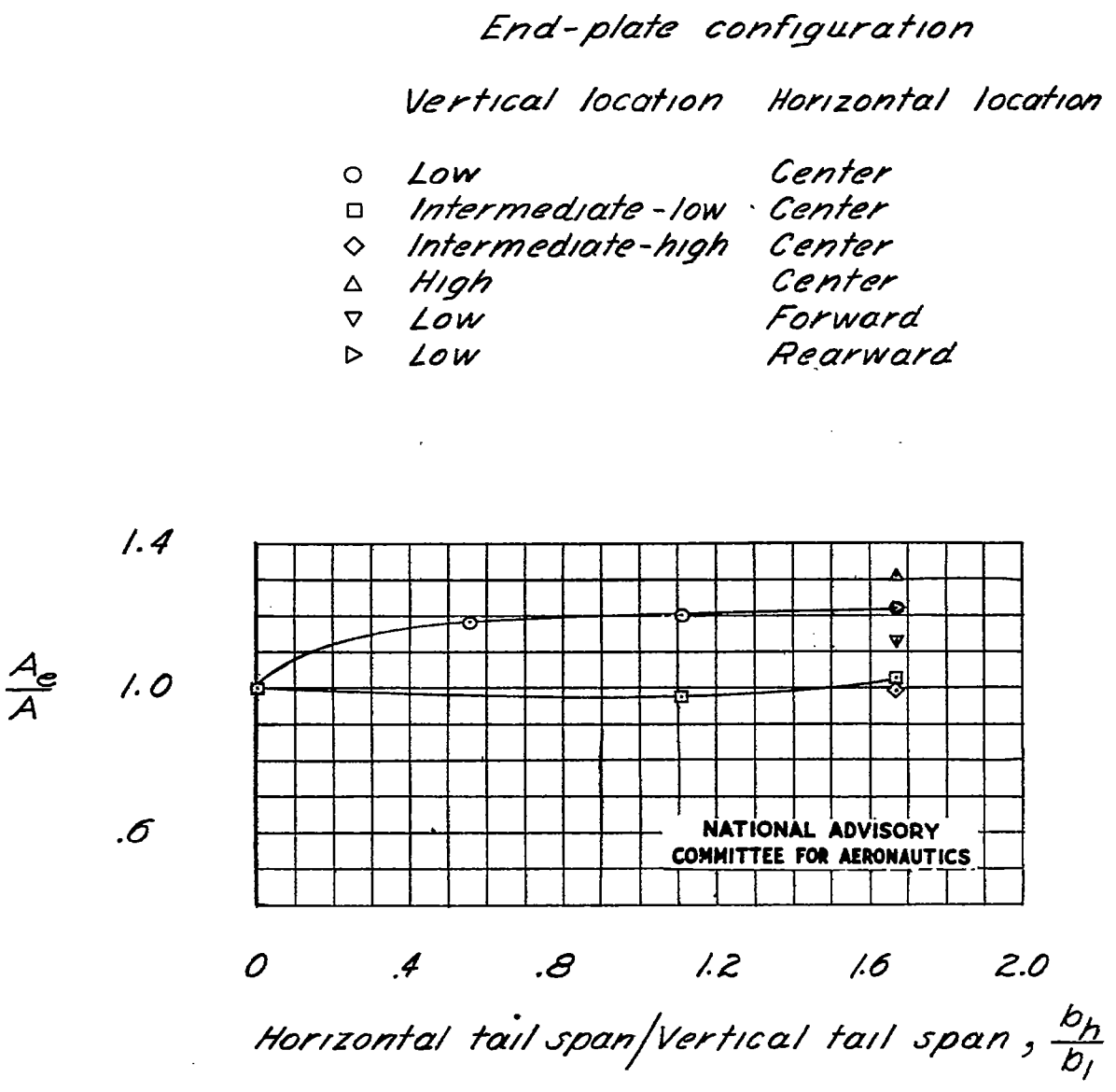


Figure 16.- Values of $A_e/A$ determined by lifting-surface theory for all model configurations. Area-span convention I.

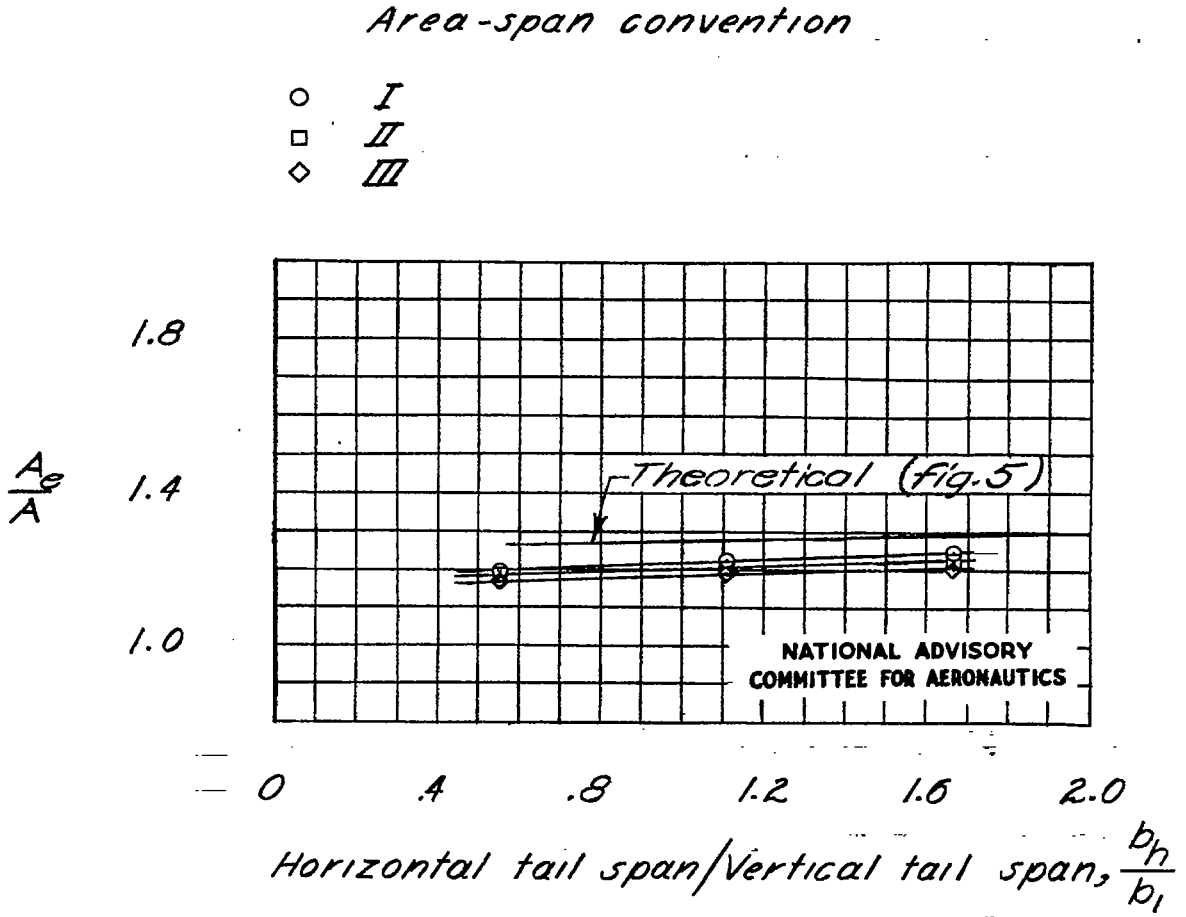


Figure 17.- Values of $A_e/A$ determined by lifting-line theory for three area-span conventions with the end plate in center horizontal location for the low vertical location.

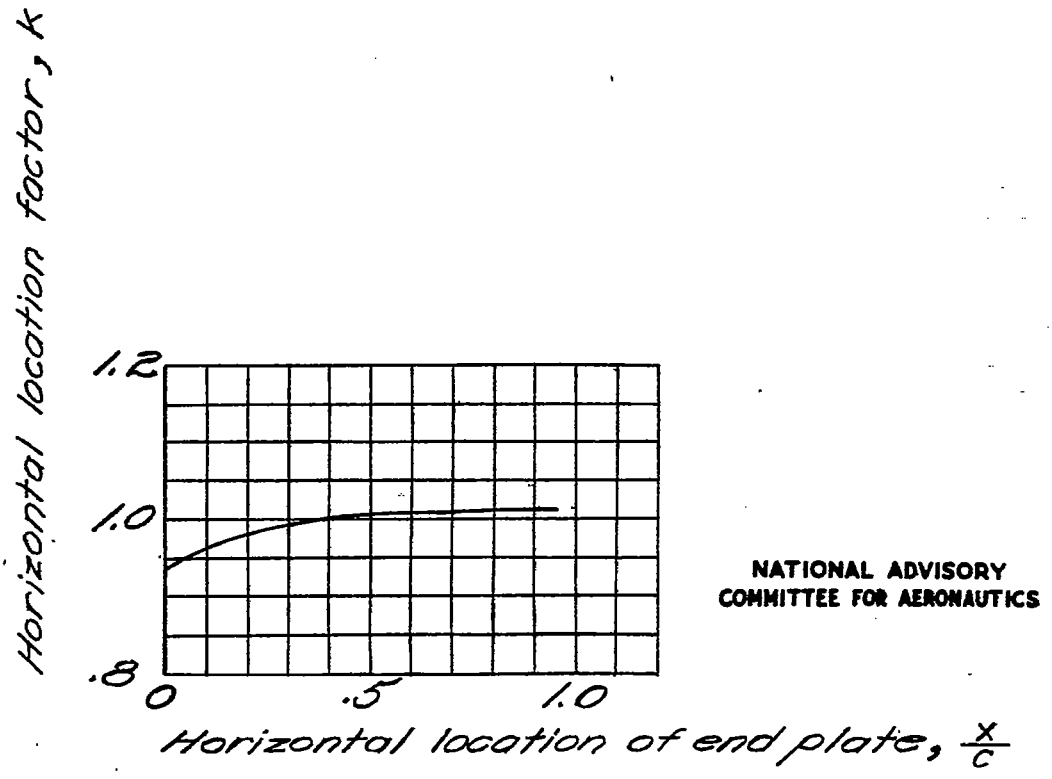


Figure 18.- Effect of end-plate horizontal location on the horizontal location factor deduced from the $C_{L_\alpha}$-data of figure 13.